CrystEngComm

Accepted Manuscript

Syntheses, structural diversity and photocatalysis properties of various Co(II) coordination polymers based on a "V"-shaped 1,3-di(4′-carboxyl-phenyl)benzene acid and different imidazole bridging ligands†

Xiang-min Meng, Chuan-bin Fan, Cai-feng Bi, Zi-ao Zong, Xia Zhang,* Yu-hua Fan*

Key Laboratory of Marine Chemistry Theory and Technology, Ministry of Education,
College of Chemistry and Chemical Engineering, Ocean University of China,
Qingdao, Shandong 266100, P.R. China

Four novel Co(II) coordination polymers (CPs) based on a "V"-shaped 1,3-di(4′-carboxyl-phenyl)benzene acid (H_2dpb), namely {[Co_2(dpb)$_2$(4,4′-bibp)$_2$]·2(CH_3CN)}$_n$(**1**), [Co(Hdpb)$_2$(4,4′-bibp)]$_n$(**2**), {[Co_2(dpb)$_2$(tib)$_2$]·H_2O}$_n$(**3**) and {[Co(dpb)(bimb)$_{0.5}$]·DMF·0.5(CH_3CN)}$_n$(**4**) (4,4′-bibp = 4,4′-bis(imidazol-1-yl)biphenyl, tib = 1,3,5 -tris(1-imidazolyl) benzene and bimb = 1,4-bis(imidazol-1-ylmethyl)benzene) have been hydrothermally synthesized and characterized by elemental analysis, IR spectra, powder X-ray diffraction (PXRD), thermogravimetric (TG) analysis and single-crystal X-ray diffraction. Single-crystal X-ray diffraction analysis exhibits that complex **1** possesses a uninodal 4-connected 3D (three-dimensional) **cds** topology framework with the Schläfli symbol ($6^5 \cdot 8$). Complex **2** shows a 1D zigzag chain, which are further assembled into a 3D supramolecular structure by O-H···O hydrogen bonds. Complex **3** shows an unprecedented 3-nodal (3,4,6)-connected 3D framework with the Schläfli symbol $(6^2 \cdot 7)^2(6^4 \cdot 7^5 \cdot 8^4 \cdot 9 \cdot 10)(6^4 \cdot 8^2)$. While complex **4** displays a {$Co_2(COO)_4$} binuclear SBUs based 3D 6-connected ($4^4 \cdot 6^{11}$)-unprecedented framework. Moreover, the photocatalytic degradation of four Co(II) compounds (complex **1**-**4**) have been investigated.

Introduction

Recently, the researches of metal-organic coordination polymers (CPs) have achieved remarkable progress because of not only their interesting topological framework and intriguing structures[1] but also their major potential applications in gas storage,[2] ion exchange,[3] magnetism,[4] heterogeneous catalysis.[5] Generally, such materials are constructed from inorganic nodes (single metal ions, polynuclear metal cluster, SBUs) and organic linkers (polycarboxylate, N-donors, phosphonate, and so on) through non-covalent interactions.[6,7] Nevertheless, the structural diversities of the designed CPs are mainly affected by two factors: one is the nature of the organic ligands (internal factors such as length, rigidity, coordination mode, functional groups and substituents) and the other one is the reaction conditions (external factors such as reaction temperature, templating agents, metal-ligand ratio, pH and counteranion).[8-11] More and more novel structures were obtained by changing the synthesis conditions. Among different conditions, the ancillary ligands are more effective to control the synthesis of CPs, which further provides inspirations to synthesis novel coordination materials.[12]

It is well known that polycarboxylate ligands with bent backbones (e.g. V-shaped, triangular, quadrangular) are excellent candidates for building highly connected, interpenetrating, or helical coordination frameworks due to their bent backbones and versatile bridging fashions.[13,14] Hence, polycarboxylates are widely utilized in the construction of CPs.[15,16] The H_2dpb not only has two carboxylate groups to bind to the metal center but also displayed a V-shaped arrangement. So the H_2dpb based CPs are also good examples for synthesis controlled CPs.

Here, we explored the coordination frameworks with 1,3-di(4′-carboxyl-phenyl)benzene acid (H_2dpb) and three auxiliary N-donor ligands [4,4′-bis(imidazol-1-yl)biphenyl (4,4′-bibp), 1,3,5- tris(1-imidazolyl) benzene (tib) and bimb = 1,4-bis(imidazol-1-ylmethyl)benzene] (Scheme 1). Subsequently we obtained four coordination polymers, namely $\{[Co_2(dpb)_2(4,4'\text{-bibp})_2]\cdot 2(CH_3CN)\}_n$(**1**), $[Co(Hdpb)_2(4,4'\text{-bibp})]_n$(**2**), $\{[Co_2(dpb)_2(tib)_2]\cdot H_2O\}_n$(**3**) and $\{[Co(dpb)(bimb)_{0.5}]\cdot DMF\cdot 0.5(CH_3CN)\}_n$(**4**) which show a systematic variation of architectures from a 1D chain based supramolecular to a 3D framework (Scheme 2). These results reveal that nature of the bridging N-donor linkers has a significant effect on the H_2dpb coordination modes and the final packing structures. Moreover, the photocatalytic activities of four Co(II) compounds (complex **1-4**) were also investigated.

Scheme 1

Scheme 2

Experimental section

Materials and physical measurements

All reagents and solvents were purchased from Jinan Henghua Sci. & Tec. Co. Ltd. and were used without further purification. The infrared spectrum was recorded as KBr pellets on the Nicolet 170SX spectrometer in the 4000-400 cm^{-1} region. Elemental analysis (C, H, and N) was performed in a model 2400 PerkinElmer analyzer. Thermogravimetric analysis (TGA) were measured on a Perkin-Elmer TGA-7 thermogravimetric analyzer under air conditions from room temperature to 800 °C with a heating rate of 10 °C min^{-1}. The X-ray powder diffractions (XRPD) were collected on an Enraf -Nonius CAD-4 X-ray single-crystal diffractometer with Cu-Kα radiation. Topological analysis was performed and confirmed by the Topos program and the Systre software.[17,18]

Synthesis of $\{[Co_2(dpb)_2(4,4'\text{-bibp})_2]\cdot 2(CH_3CN)\}_n$(1)

A mixture of H_2dpb (0.20 mmol, 0.064 g), 4,4′-bibp (0.20 mmol, 0.058 g), and $Co(NO_3)_2\cdot 6H_2O$ (0.20 mmol, 0.058 g) was dissolved in 8 mL of CH_3CN/H_2O (3:1, v/v). The final mixture was placed in a Teflon-lined stainless steel vessel, heated to 150 °C for 3 days, and then cooled (a descent rate of 5 °C h^{-1}) to room temperature. Purple block crystals of **1** were obtained. Yield of 53% (based on Co). Anal. (%) calcd. for $C_{80}H_{58}Co_2N_{10}O_8$: C, 68.38; H, 4.16; N, 9.97. Found: C, 68.16; H,4.11; N, 9.88. IR (KBr pellet, cm^{-1}): 3140 (w), 1608 (m), 1511 (s), 1391 (vs), 1311 (m), 817 (m), 777 (m).

Synthesis of $[Co(Hdpb)_2(4,4'\text{-bibp})]_n$(2)

A mixture of H_2dpb (0.20 mmol, 0.064 g), 4,4′-bibp (0.20 mmol, 0.058 g), $Co(NO_3)_2\cdot 6H_2O$ (0.20 mmol, 0.058 g), NaOH (0.40 mmol, 0.016 g) and 8 mL of water was placed in a Teflon-lined stainless steel vessel, heated to 150 °C for 3 days, and then cooled (a descent rate of 5 °C h^{-1}) to room temperature. Pink block crystals of **2** were obtained. Yield of 51% (based on Co). Anal. (%) calcd. for $C_{58}H_{40}CoNO_8$: C, 74.28; H, 4.29; N, 1.49. Found: C, 73.99; H, 4.31; N, 1.46. IR (KBr pellet, cm^{-1}): 3123 (m), 1600 (s), 1515 (s), 1390 (vs), 1306 (m), 821 (m), 776 (s).

Synthesis of $\{[Co_2(dpb)_2(tib)_2]\cdot H_2O\}_n$(3)

A mixture of H_2dpb (0.20 mmol, 0.064 g), tib (0.20 mmol, 0.056 g), $Co(NO_3)_2\cdot 6H_2O$ (0.20 mmol, 0.058 g), NaOH (0.40 mmol, 0.016 g) and 8 mL of water was placed in a Teflon-lined stainless steel vessel, heated to 150 °C for 3 days, and then cooled (a descent rate of 5 °C h^{-1}) to room temperature. Violet block crystals of **3** were obtained. Yield of 42% (based on Co). Anal. (%) calcd. for $C_{70}H_{52}Co_2N_{12}O_{10}$: C, 67.56; H, 4.18; N, 8.29. Found: C, 67.33; H, 4.26; N, 8.18. IR (KBr pellet, cm^{-1}): 3395 (w), 3142 (w), 1599 (w), 1498 (s), 1384 (vs), 1237 (w), 775 (w), 734 (w).

Synthesis of $\{[Co(dpb)(bimb)_{0.5}]\cdot DMF\cdot 0.5(CH_3CN)\}_n$(4)

A mixture of H_2dpb (0.20 mmol, 0.064g), bimb (0.20 mmol, 0.048g), $Co(NO_3)_2\cdot 6H_2O$ (0.20 mmol, 0.058 g) and 8 mL of DMF-CH_3CN (v/v=1:1) were placed in a Teflon-lined stainless steel vessel, heated to 150 °C for 3 days, and then cooled (a descent rate of 5 °C h^{-1}) to room temperature. Purple block crystals of **4** were obtained. Yield of 51% (based on Co). Anal. (%) calcd. for $C_{63}H_{59}Co_2N_7O_{11}$: C, 62.63; H, 4.92; N, 8.11. Found: C, 62.38; H, 4.95; N, 8.03. IR (KBr pellet, cm^{-1}): 3688 (m), 3110 (m), 1605 (s), 1530 (m), 1380 (vs), 1101 (m), 855 (m), 781 (m) 662 (w).

X-ray crystallography

Single crystals of the complexes **1-4** with appropriate dimensions were chosen under an optical microscope and quickly coated with high vacuum grease (Dow Corning Corporation) before being mounted on glass fiber for data collection. X-ray crystallography data of complexes **1-4** were collected on a Bruker Apex Smart CCD diffractometer at 293(2) K with graphite-monochromatized Mo-Kα radiation (λ = 0.71073 Å) by using the ω-2ɵ scan mode. A preliminary orientation matrix and unit cell parameters were determined from 3 runs of 12 frames each, each frame corresponding to a 0.5° scan in 5 s, followed by spot integration and least-squares refinement. For complexes **1-4**, the data were measured using scans of 0.5° per frame for 10 s until a complete hemisphere had been collected. Cell parameters were retrieved using the SMART software and refined using SAINT on all observed reflections.[19] Data reduction was performed using the SAINT software and corrected for Lorentz and polarization effects. Absorption corrections were applied using the program SADABS.[19] In all cases, the highest symmetry was chosen. The structure was solved by direct methods using SHELXS-97.[20] The non-hydrogen atoms were defined by the Fourier synthesis method. Positional and thermal parameters were refined by the full matrix least-squares method (on F^2) to convergence.[21] Hydrogen atoms were placed at calculated positions and included as riding atoms with isotropic displacement parameters 1.2-1.5 times U_{eq} of the attached C atoms. All structures were examined using the Addsym subroutine of PLATON[22] to ensure that no additional symmetry could be applied to the models. Crystallographic data for complexes **1-4** are given in Table 1. Selected bond lengths and angles for **1-4** are listed in Table S1.† CCDC numbers for complexes of **1-4** are 1062888 for **1**, 1061112 for **2**, 1402588 for 3 and 1434301 for 4.

Table 1

Results and discussion

Synthesis and characterization

The synthesis of complexes **1-4** was constructed from H_2dpb and the related Co(II) salt in the presence of three N-donor (4,4′-bibp, tib, bimb) bridging linkers under hydrothermal condition. Those complexes **1-4** are stable in the solid state even after extended exposure to air. Meanwhile, all of the complexes **1-4** have poor solubility in water and common organic solvent, but can be slightly soluble in very high polarity solvents.

Structure description of $\{[Co_2(dpb)_2(4,4'\text{-bibp})_2]\cdot 2(CH_3CN)\}_n$(1)

The crystal structure determined by single-crystal X-ray diffraction showed that complex **1** crystallizes in the monoclinic system, space group $P2_1/c$. As can be seen from Fig. 1a, the asymmetric unit of **1** contains two types Co^{II} ions (Co1 and Co2), two dpb^{2-} ligands and two 4,4′-bibp ligands. Each of the Co^{II} ions shows a hexa-coordinated, completed by four oxygen atoms from three different dpb^{2-} ligands and two nitrogen atoms from two individual 4,4′-bibp ligands, resulting in a distorted octahedral coordination geometry. The bond lengths of Co-O and Co-N are in the range 2.021(4)-2.224(5) Å and 2.109(5)-2.159(5) Å, respectively. Both Co-O and Co-N bond length are well-matched to similar complexes.[23]

The H_2dpb ligand in complex **1** is completely deprotonated and exhibits a μ_3-(κ^1-κ^1)-(κ^1-κ^1) coordination mode (Scheme 3, Mode III). The dihedral angles between the three phenyl rings in dpb^{2-} are 41.52(9), 41.96(6) and 43.63(7)°, respectively. Two Co1 ions are connected by the μ_2-(κ^1-κ^1) carboxyl group, forming $\{Co_2(COO)_2\}^1$ SBUs, which can be viewed as the shared nodal. Interestingly, the Co2 were connected by the same mode compared with Co1, forming $\{Co_2(COO)_2\}^2$ SBUs (Fig. 1b). The two same $\{Co_2(COO)_2\}$ SBUs are connected by dpb^{2-} and 4,4′-bibp ligands, forming a stable 3D framework (Fig. 1c). The distances separated by dpb^{2-} and 4,4′-bibp between adjacent SBUs ($\{Co_2(COO)_2\}^1\cdots\{Co_2(COO)_2\}^2$) are 16.563 Å and 17.936 Å, respectively. Then from the final 3D framework, we can find that the bis(imidazole) is the most important linker which linked the adjacent $[Co(dpb)]_n$ chain and as pillars to support the framework. Moreover, with the guest CH_3CN molecules being omitted, calculation PLATON shows that the void volume of **1** is 12.1% of the crystal volume (798.0 out of the 6615.7 $Å^3$ unit cell volumes).[24]

From the viewpoint of topology, the final obtained 3D structure exhibits as an uninodal **cds** 4-connected 3D framework with the point Schläfli symbol ($6^5 \cdot 8$) by denoting $\{Co_2(COO)_2\}^1$and $\{Co_2(COO)_2\}^2$ SBUs as 4-connected nodes (Fig. 1d).

Fig. 1 (a-d)

Scheme 3

Structure description of $[Co(Hdpb)_2(4,4'\text{-bibp})]_n$(2)

A similar reaction environment compared with complex **1** was used except for the H_2O-CH_3CN system being replaced with the H_2O, resulting in a 3D supramolecular structure. Complex **2** crystallizes in monoclinic space group *C*2/c. The asymmetric unit of **2** contains one Co^{II} ion, two $Hdpb^-$ carboxylate ligands, and one 4,4′-bibp N-donor ligand as shown in Fig. 2a. The Co1 center is a four-coordinated by two O atoms from two $Hdpb^-$ ligands and two N atoms from two 4,4′-bibp ligands, displaying a distorted triangle cone geometry. The bond length of Co-O is 1.944(3) Å, and the Co-N distance is 2.047(4) Å, respectively. Both Co-O and Co-N bond length also well-matched to similar complexes.[23]

The two partially deprotonated carboxyl groups of $Hdpb^-$ ligands exhibit a μ_1-(κ^1-κ^0) coordination mode (Scheme 3, Mode I) linking the same Co^{II} ion, and the N-donor ligands linking two neighboring Co^{II} ions along the axis to form a 1D zigzag chain $[Co(bibp)]_n$ (Fig. 2b). Such chains are linked through O-H···O hydrogen bonds along [1,1,0] orientation to form 3D cone supramolecular structure (Fig. 2c). The dihedral angle between the three phenyl rings in $Hdpb^-$ are 20.87(6)°, 34.16(6)° and 47.50(7)° respectively.

Fig. 2 (a-c)

Structure description of $\{[Co_2(dpb)_2(tib)_2]\cdot H_2O\}_n$(3)

For the purpose of exploring new materials, the tris(imidazole) linker (tib) was employed in the reaction system, and an unprecedented 3D framework was obtained. Structure analysis reveals that complex **3** crystallizes in the Monoclinic system, space group *C*2/c. The asymmetric unit of **3** contains two Co^{II} ions (Co1 and Co2), two dpb^{2-} ligands, and two tib ligands. As shown in Fig. 3a, the environment around Co1 can be described as a slightly distorted octahedron geometry, coordinated by four N atoms from four different tib ligands and two O atoms from two different dpb^{2-} ligands with a $\{CoN_4O_2\}$ coordination environment. Oppositely, each Co2 coordinated by four O atoms from four different dpb^{2-} ligands and two N atoms from two different tib ligands, forming a distorted octahedron geometry with a $\{CoN_2O_4\}$ coordination environment. The bonds lengths of Co-O and Co-N are in the range 1.948(3)-2.083(2) Å and 2.049(3)-2.167(3) Å, respectively. Additionally, the Co···Co distances separated by dpb^{2-} is 17.473(11) Å in **3**.

The H_2dpb in complex **3** is completely deprotonated and exhibits a μ_2-(κ^1-κ^1)-(κ^1-κ^0) coordination mode (Scheme 3, Mode II). The Co^{II} cations are bridged by μ_3-*tib* N-donor ligands to generate an unprecedented 2-nodal (3,4)-connected 3D framework with $(6^2\cdot8^2\cdot10^2)(6^2\cdot8)^2$ topology (Fig. 3b). This framework is further linked by dpb^{2-} ligands to generate a more complicated 3D framework (Fig. 3c). The effective free volume of **3** was 6.0% of the crystal volume (356.3 out of the 5906.4 $Å^3$ unit cell volumes), calculated by PLATON analysis.

From the viewpoint of structural topology, the whole 3D structure exhibits an unprecedented 3-nodal (3,4,6)-connected 3D framework with $(6^2\cdot7)^2(6^4\cdot7^5\cdot8^4\cdot9\cdot10)(6^4\cdot8^2)$ topology (Fig. 3d).

Fig. 3 (a-d)

Structure description of $\{[Co(dpb)(bimb)_{0.5}]\cdot DMF\cdot0.5(CH_3CN)\}_n$(4)

In order to obtain more flexible MOFs, the flexible bis(imidazole) linker (bimb) was employed in the same reaction system. The crystal structure determined by single-crystal X-ray diffraction showed that complex **4** crystallizes in the monoclinic system, space group *C*2/*c*. As can be seen from Fig. 4a, the asymmetric unit consists of one Co^{II} ion, one dpb^{2-} carboxylate ligands, and a half of bimb N-donor ligand. The two symmetrically equivalent Co1 and Co1a ions are bridged by four μ_2-(κ^1-κ^1) carboxylate groups to form a binuclear Co^{II} carboxylate cluster with a separation of 2.840(12) Å for Co1-$Co1^{\#1}$ (symmetry codes: #1: -x + 3/2, -y + 3/2,-z + 1)(Table S1

†), which can be viewed as the shared $\{Co_2(COO)_4\}$ SBUs. Every one of the Co(1) center is a penta-coordinated by one N atoms from a bimb bridging linker and four O atoms from four dpb^{2-} ligands, displaying a slightly distorted tetrahedral coordination geometry. The bond lengths of Co-N and Co-O are in the range 1.970(18)-2.060(12) Å and 2.012(4)-2.068(4) Å, respectively. Interestingly, the Co···Co distances separated by dpb^{2-} is 17.080(11) Å in **4**, and similar with **3** (17.473(11) Å).

In complex **4**, the H_2dpb ligand is completely deprotonated and exhibits a μ_4-(κ^1-κ^1)-(κ^1-κ^1) coordination mode (Scheme 3, Mode IV). Each $\{Co_2(COO)_4\}$ SBUs is connected with four dpb^{2-} anions, constructing a 2D 4-connected $(4^4 \cdot 6^2)$-**sql** network (Fig. 4b). The 2D networks are linked by bimb ligands to generate a stable 3D framework (Fig. 4c). Particularly, only half the bimb ligands act as pillars to support the framework, and the excess bimb ligands coordinate terminally with $\{Co_2(COO)_4\}$ SBUs to support the stability of the final structure. Besides, the void volume in **4** is 30.0% of the crystal volume (1773.7 out of the 5905.5 Å^3 unit cell volume), calculated by PLATON.

The topology analysis shows that the overall structure of complex **4** can be defined as an unprecedented uninodal 6-connected 3D framework with $(4^4 \cdot 6^{11})$ topology (Fig. 4d).

Fig. 4 (a-d)

Structural comparison and discussion

The structures of coordination networks in MOFs have been found to be greatly influenced by central metals, solvent and N-donor ligands. As shown in Scheme 3 and Table S2 †, H_2dpb exhibits versatile coordination modes, resulting in different new topologies. In complexes **1** and **3**, the dpb^{2-} ligands allow them to chelate the metal atoms (chelate and bidentate in **1** and chelate and monodentate in **3**) through their two carboxylate groups, to further stabilize 1D chain. Then those 1D liner chains are further interacted with 4,4′-bibp and tib ligands to formed the final 4-connected **cds** and (3,4,6)-connected unprecedented 3D topologies. For **2**, only one carboxylate group of H_2dpb ligands coordinated with metal atoms (monodentate in **2**), and the last carboxylate group interacted with adjacent $[Co(Hdpb)_2(4,4'\text{-bibp})]_n$ chain to formed the 3D supramolecular structure through the H-bonding interactions. For **4**, carboxylate groups of dpb^{2-} adopt bidentate coordination fashions, connecting neighboring Co^{II} atoms to form the 2D network, which is further bridged by the bimb ligands to form a 3D 6-connected frameworks. Meanwhile, H_2dpb is completed deprotonated in **1**, **3** and **4**, and partly deprotonated ($Hdpb^{-}$) in **2**, and their asymmetric units contain two dpb^{2-} ligands, except **2** contain one $Hdpb^{-}$ ligand. All of the H_2dpb ligands connect one (**2**), two (**3**), three (**1**), or four (**4**) metal ions in their 3D polymeric structures. Hence, the metal centers Co^{II} show 4-coordinated triangle cone, 5-coordinated tetrahedral and 6-coordinated octahedral geometries, respectively.

For N-donor ligands, the differences of their lengths, substituent groups and configurations greatly influence the final structure of the targeted CPs. In **1**, **2** and **4**, not only N-donor auxiliary ligands adopt similar μ_2 bridging coordination modes, but also their spatial orientations are quite similar (anti-conformation). It is shown that the flexibility of C linkage can make a contribution to the spatial orientations of imidazole in **4**. For **3**, influence by the rigid of the benzene ring, the tib displays syn-conformation. Due to the different configuration of the N-donor ligands, the **4** show a higher effective free volume (30.0%) than complexes **1** (12.1%) and **3** (6.0%). Hence, complex **4** may be a good candidate for application in gas absorption.

Minor changes could induce large influences in designed MOFs. The different coordination modes indicate that the different imidazole ancillary linkers give different preferences in the coordination with metal or metal cluster based SBUs, and finally construct stable complexes. The solvent system also has a great effect on the diversity of the final architectures. Our four target structures are the result of multiple factors.

Thermal analyses

Thermogravimetric (TG) analysis of complexes **1- 4** was performed on polycrystalline samples of **1-4** in an N_2 atmosphere with a heating rate of 10 °C min^{-1} and the results are shown in Fig. 5. For complex **1**, first weight loss in the temperature range of 130-260 °C is consistent with the removal of the lattice CH_3CN (obsd: 5.5%, calcd: 5.8%). The second weight loss corresponds to the loss of the organic ligands in 350 °C. For complex **2**, the whole structure starts to collapse at about 300 °C with a result of thermal decomposition (observed: 11.2%, calcd: 10.5%). For **3**, the weight loss of water molecules is observed in the range of 70-160 °C (obsd: 2.5% and calcd: 2.7%). The decomposition of organic ligands start at 375 °C. For complex **4**, the overall structure is stable up to 360 °C, and then the decomposition of organic ligands begins, finally giving a residual weight in 800 °C (obsd: 29.5% and calcd: 6.2%).

Fig. 5

Photocatalysis properties

Rhodamine B (RhB) and methylene violet (MV) are the most common organic dyes in waste water, and it is well known that CPs often show photocatalytic activity in the degradation of some organic dyes under UV irradiation by oxidation of organic materials.[25] Meanwhile, Wang's group has prepared six Co(II) complexes based on the bis-pyridyl-bis-amide derivative, which show photocatalytic activity towards the degradation of methylene blue (MB) under UV irradiation.[26] However, the photocatalytic activity of rhodamine B (RhB) and methylene violet (MV) under UV irradiation has not been reported yet. Herein we perform photocatalytic tests of the title complexes towards the degradation of RhB and MV under UV irradiation. The photocatalytic reactions were performed by a typical process[27]: 20 mg of **1**, **2**, **3** or **4** was dispersed in 90 mL aqueous solution of RhB (6 mg L^{-1}) or MV (6 mg L^{-1}), respectively. The mixture containing organic dye and the title compound was magnetically stirred in the dark for 30 min till an adsorption-desorption equilibrium was established, before turning on the Hg lamp (125 W). Then 5 mL samples were taken out regularly from the photocatalytic reactor and centrifuged immediately for separation of any solid. The transparent solution was tested under UV measurement.[28]

The photocatalytic behaviors of complexes **1-4** in RhB solution were shown in Fig. 6. From the Fig. 6a-d, we can found that the absorbance peaks of RhB decreased obviously with different photocatalytic efficiency when the compounds were added. Moreover, the concentration ratios of RhB (c_0/c) against irradiation time (min) in the presence of the complexes **1-4** were plotted, with c representing the initial concentration of RhB after magnetically stirring in the dark for 30 min (Fig. 6e). For complexes **1-4**, the RhB solution has been taken out every 20 min, but the photocatalytic efficiency is different. The degradation ratios of RhB are 96.2% for **1**, 88.1% for **2**, 90.3% for **3** and 60.9% for **4** after 120 min of UV irradiation, and the photocatalytic activity is **1** > **3** > **2** > **4**. Meanwhile, all the RhB degradation ratios of control experiments did not surpass 30% and nearly cease after 120 min under UV irradiation.

As shown in Fig. 7, the degradation ratios of MV are 90 % for **1**, 90.1% for **2**, 90.1 % for **3** and 59.3 % for **4** after 70 min of UV irradiation. The MV degradation ratios of control experiments did not surpass 30% and nearly cease after 70 min under UV irradiation. The photocatalytic activity of the complex **1**, **2** and **3** are similar, but much better than complex **4**. Moreover, the photocatalytic activity of the complex **1**, **2**, **3** and **4** are better in MV solution compared with RhB solution in 70 min (Fig. 8).

All the degradation activity results show that compared with compound **1**, **2** and **3**, compound **4** has weak photocatalytic activities for the photodegradation of RhB and MV under UV irradiation. As we known, complex structures such as the numbers of the coordinated water molecules, the coordination environments of the central metals, the extent of the conjugation[29] and the sizes of the metal-oxygen clusters,[30] are the main factors that influence their photocatalytic activities. Although the composite of **4** is greatly related to that of **1**, the number of their water molecules, the coordination environments of their central metals, and the sizes of their Co-oxygen clusters are entirely different.[31] For example, compound **1** contains the binuclear $[Co_2(COO)_2]$ (Co(1)···Co(1) = 4.522(13) and Co(2)···Co(2) = 4.679(12)) units, while compound **4** possesses the binuclear $[Co_2(COO)_4]$ (Co···Co = 2.840(12)) units. Therefore, it can be surmised that the relatively large binuclear $[Co_2(COO)_2]$ units of **1** aid in the transport of excited holes/electrons to the surface to initiate the photocatalytic decomposition reaction with RhB and MV.[30] Moreover, three of the titled Co(II) compounds (**1-3**) show better photocatalytic activities compared with other reported CPs ($[Cu_3(4\text{-atrz})_8(PMo_{12}O_{40})_2(H_2O)_2]\cdot 2H_2O$[32] and $\{[Cu_3(H_3tpb)_2(tpb)(Mo_4O_{12})]\cdot 4H_2O\}_n$[33]) in the degradation of RhB and MV under the same condition. The results indicate that complexes **1-3** show good photocatalytic activity for the degradation of RhB and MV, and may be candidates for photocatalytic activity in the degradation of some organic dyes.

Complexes **1-4** involve both N and O coordinating atoms. It is known that when the complex is exposed to UV light (photo-excitation), there is an electron transfer from the highest occupied molecular orbital (HOMO) contributed by the oxygen and/or nitrogen 2p bonding orbital (valence band) to the lowest unoccupied molecular orbital (LUMO) contributed by an empty metal orbital (conduction band). The HOMO strongly demands one electron to return to its stable state. Thus, one electron is captured from the water molecule, which is oxygenated into the ·OH radical. Meanwhile, the ·OH groups allow the adsorption of O_2 from water, and the photo formed electrons reduce O_2 to O_2^- species, which in turn can interact with water to form further oxygenated radicals (mainly hydroxyl radicals ·OH).[34] The ·OH active species could decompose RhB/MV effectively to complete the photocatalytic process.[35]

In order to investigate the stability of the complexes **1-4**, the PXRD patterns of the recycled powder were obtained, shown in Fig. S1 †. The PXRD results reveal that four Co(II) compounds were stable in degradation process.

Fig. 6 (a-e)

Fig. 7 (a-e)

Fig. 8

Conclusions

In summary, four CPs were synthesized based on 1,3-di(4′-carboxyl-phenyl)benzene acid (H_2dpb) and three different imidazole bridging linkers (4,4′-bibp, bimb, tib) under hydrothermal conditions, with the final packing structures exhibiting a systematic variation of architectures from 1D chains based supramolecular to 3D frameworks. These results reveal that nature of the bridging N-donor linkers have significant effects on the H_2dpb coordination modes and the final packing structures. Moreover, the photocatalytic studies indicate three Co(II) compounds (complex **1**, **2** and **3**) are good candidates for the photocatalytic degradation of rhodamine B (RhB) and methylene violet (MV).

Acknowledgements

This research was supported by the National Natural Science Foundation of China to C.F. Bi (No. 21371161 and No. 21071134), the Specialized Research Fund for the Doctoral Program of Higher Education of China (No. 20120132110015), the Natural Science Foundation of Shandong Province to X. Zhang (No. ZR2012BQ026).

References

1 (a) Z. Z. Lu, R. Zhang, Y. Z. Li, Z. J. Guo, H. G. Zheng, *Chem. Commun.*, 2011, 47, 2919; (b) J. J. Perry, J. A. Perman, M. J. Zaworotko, *Chem. Soc. Rev.*, 2009, 38, 1400; (c) D. J. Tranchemontagne, Z. H. Ni, M. O'Keeffe, O. M. Yaghi, *Angew. Chem., Int. Ed.*, 2008, 47, 5136; (d) C. N. R. Rao, S. Natarajan, R. Vaidhyanathan, *Angew. Chem., Int. Ed.*, 2004,43,1466; (e) S. R. Batten, R. Robson, *Angew. Chem., Int. Ed.*, 1998, 37, 1460.

2 (a) M. O'Keeffe and O. M. Yaghi, *Chem. Rev.*, 2012, 112, 675; (b) B. L. Chen, N. W. Ockwig, A. R. Millward, D. S. Contreras and O. M. Yaghi, *Angew. Chem., Int. Ed.*, 2005, 44, 4745; (c) Y. Cui, Y. Yue, G. Qian and B. L. Chen, *Chem. Rev.*, 2012, 112, 1126; (d) G. Férey and C. Serre, *Chem. Soc. Rev.*, 2009, 38, 1380; (e) Z. Chen, R. Wang and J. Li, *Chem. Mater.*, 2000, 12, 762; (f) M. Kim, J. F. Cahill, H. Fei, K. A. Prather and S. M. Cohen, *J. Am. Chem. Soc.*, 2012, 134, 18082; (g) H. Fei, J. F. Cahill, K. A. Prather and S. M. Cohen, *Inorg. Chem.*, 2013, 52, 4011.

3 (a) J. An, S. J. Geib, N. L. J. Rosi, *Am. Chem. Soc.*, 2009, 131, 8376; (b) F. Nouar, J. Eckert, J. F. Eubank, P. Forster, M. J. Eddaoudi, *Am. Chem. Soc.*, 2009, 131, 2864.

4 (a) L. L. Johnston, J. H. Nettleman, M. A. Braverman, L. K. Sposato, R. M. Supkowski, R. L. LaDuca, *Polyhedron.*, 2010, 29, 303; (b) Z. R. Pan, H. G. Zheng, T. W. Wang, Y. Song, Y. Z. Li, Z. J. Guo, S. R. Batten, *Inorg. Chem.*, 2008, 47, 9528; (c) S. M. Humphrey, P. T. J. Wood, *Am. Chem. Soc.*, 2004, 126, 13236; (d) E. K. Brechin, S. G. Harris, A. Harrison, S. Parsons, A. G. Whittaker, R. E. P. Winpenny, *Chem. Commun.*, 1997, 653.

5 (a) F. Cao, S. Wang, D. Li, S. Zeng, M. Niu, Y. Song and J. Dou, *Inorg. Chem.*, 2013, 52, 10747; (b) X. T. Zhang, D. Sun, B. Li, L. M. Fan, B. Li and P. H. Wei, *Cryst. Growth Des.*, 2012, 12, 3845; (c) J. B. Lin, W. Xue, B. Y. Wang, J. Tao, W. X. Zhang, J. P. Zhang and X. M. Chen, *Inorg. Chem.*, 2012, 51, 9423; (d) T. Liu, S. N. Wang, J. Lu, J. M. Dou, M. J. Niu, D. C. Li and J. F. Bai, *CrystEngComm*, 2013, 15, 5476; (e) X. Zhang, L. Fan, W. Zhang, Y. Ding, W. Fan and X. Zhao, *Dalton Trans.*, 2013, 42, 16562; (f) P. V. Dau and S. M. Cohen, *Chem. Commun.*, 2013, 49, 6128.

6 (a) S. Chen, R. Shang, K. L. Hu, Z. M. Wang and S. Gao, *Inorg. Chem. Front.*, 2014, 1, 83; (b) Y. Wang, H. X. Lin, L. Chen, S. Y. Ding, Z. C. Lei, D. Y. Liu, X. Y. Cao, H. J. Liang, Y. B. Jiang and Z. Q. Tian, *Chem. Soc. Rev.*, 2014, 43, 399; (c) H. Zhou, G. X. Liu, X. F. Wang and Y. Wang, *CrystEngComm*, 2013, 15, 1377; (d) S. Y. Song, X. Z. Song, S. N. Zhao, C. Qin, S. Q. Su, M. Zhu, Z. M. Hao and H. J. Zhang, *Dalton Trans.*, 2012, 41, 10412.

7 (a) L. Li, J. Ma, C. Song, T. Chen, Z. Sun, S. Wang, J. Luo and M. Hong, *Inorg. Chem.*, 2012, 51, 2438; (b) C. C. Ji, J. Li, Y. Z. Li, Z. J. Guo and H. G. Zheng, *CrystEngComm*, 2011, 13, 459; (c) D. Sun, L. L. Han, S. Yuan, Y. K. Deng, M. Z. Xu and D. F. Sun, *Cryst. Growth Des.*, 2013, 13, 377; (d) X. Zhang, L. Fan, Z. Sun, W. Zhang, W. Fan, L. Sun and X. Zhao, *CrystEngComm*, 2013, 15, 4910.

8 (a) X. H. Chang, J. H. Qin, M. L. Han, L. F. Ma and L. Y. Han, *CrystEngComm*,

2014, 16, 870; (b) N. Zhang,Y. Tai, M. Liu, P. Ma, J. Zhao and J. Niu, *Dalton Trans.*, 2014, 43, 5182; (c) W. Meng, Z. Xu, J. Ding, D. Wu, X. Han, H. Hou and Y. Fan, *Cryst. Growth Des.*, 2014, 14, 730; (d) L. Fan, X. Zhang, D. Li, D. Sun, W. Zhang and J. Dou, *CrystEngComm*, 2013, 15, 349.

9 (a) J. J. Wang, T. T. Wang, L. Tang, X. Y. Hou, M. L. Zhang, L. J. Gao, F. Fu and Y. X. Ren, *Z. Anorg. Allg. Chem.*, 2014, 640, 483; (b) Y. B. Wang, Y. L. Lei, S. H. Chi and Y. J. Luo, *Dalton Trans.*, 2013, 42, 1862; (c) Q. Yu, Q. Zhang, H. Bian, H. Liang, B. Zhao, S. Yan and D. Liao, *Cryst. Growth Des.*, 2008, 8, 1140; (d) X. Zhang, L. Fan, Z. Sun, W. Zhang, D. Li, J. Dou and L. Han, *Cryst. Growth Des.*, 2013, 13, 792.

10 (a) G. L. Liu and H. Liu, *CrystEngComm*, 2013, 15, 6870; (b) C. Zhan, C. Zou, G. Q. Kong and C. D. Wu, *Cryst. Growth Des.*, 2013, 13, 1429; (c) J. J. Wang, T. T. Wang, L. Tang, X. Y. Hou, L. J. Gao, F. Fu and M. L. Zhang, J. *Coord. Chem.*, 2013, 66, 3979; (d) L. Fan, X. Zhang, Z. Sun, W. Zhang, Y. Ding, W. Fan, L. Sun, X. Zhao and H. Lei, *Cryst. Growth Des.*, 2013, 13, 2462.

11 (a) Q. L. Zhang, G. W. Feng, Y. Q. Zhang and B. X. Zhu, *RSC Adv.*, 2014, 4, 11384; (b) B. Guo, L. Li, Y. Wang, Y. Zhu and G. Li, *CrystEngComm*, 2013, 42, 14268; (c) M. L. Han, S. C. Wang and D. F. Feng, *Cryst. Res. Technol.*, 2014, 49, 276; (d) Q. L. Zhang, P. Hu, Y. Zhao, G. W. Feng, Y. Q. Zhang, B. X. Zhu and Z. Tao, *J. Solid State Chem.*, 2014, 210, 178.

12 (a) F. Guo, B. Zhu, M. Liu, X. Zhang, J. Zhang and J. Zhao, *CrystEngComm*, 2013, 15, 6191; (b) L. Fan, X. Zhang, W. Zhang, Y. Ding, W. Fan, L. Sun, Y. Pang and X. Zhao, *Dalton Trans.*, 2014, 43, 6701; (c) X. Zhang, L. Fan, W. Zhang, W. Fan, L. Sun and X. Zhao, *CrystEngComm*, 2014, 16, 3203; (d) B. Liu, L. Wei, N. N. Li, W. P. Wu, H. Miao, Y. Y. Wang and Q. Z. Shi, *Cryst. Growth Des.*, 2014, 14, 1110.

13 (a) X. Lin, I. Telepeni, A. J. Blake, A. Dailly, C. M. Brown, J. M. Simmons, M. Zoppi, G. S. Walker, K. M. Thomas, T. J. Mays, P. Hubberstey, N. R. Champness and M. Schröder, *J. Am. Chem. Soc.*, 2009, 131, 2159; (b) H. S. Choi and M. P. Suh, *Angew. Chem., Int. Ed.*, 2009, 48, 6865; (c) B. L. Chen, N. W. Ockwig, A. R. Millward, D. S. Contreras and O. M. Yaghi, *Angew. Chem., Int. Ed.*, 2005, 44, 4745; (d) J. Jia, X. Lin, C. Wilson, A. J. Blake, N. R. Champness, P. Hubberstey, G. Walker, E. J. Cussen and M. Schroder, *Chem. Commun.*, 2007, 840.

14 (a) J. M. Lim, P. Kim, M. C. Yoon, J. Sung, V. Dehm, Z. J. Chen, F. Wurthner and D. Kim, *Chem. Sci.*, 2013, 4, 388; (b) F. Guo, F. Wang, H. Yang, X. L. Zhang and J.

Zhang, *Inorg. Chem.*, 2012, 51, 9677; (c) D. R. Xiao, Y. G. Li, E. B. Wang, L. L. Fan, H. Y. An, Z. M. Su and L. Xu, *Inorg. Chem.*, 2007, 46, 4158; (d) S. N. Wang, R. R. Yun, Y. Q. Peng, Q. F. Zhang, J. Lu, J. M. Dou, J. F. Bai, D. C. Li and D. Q. Wang, *Cryst. Growth Des.*, 2012, 12, 79.

15 (a) S. Y. Yang, L. S. Long, Y. B. Jiang, R. B. Huang and L. S. Zheng, *Chem. Mater.*, 2002, 14, 3229; (b) X. Guo, G. Zhu, Z. Li, F. Sun, Z. Yang and S. Qiu, *Chem. Commun.*, 2006, 3172; (c) W.-X. Chen, S.-T. Wu, L.-S. Long, R.-B. Huang and L.-S. Zheng, *Cryst. Growth Des.*, 2007, 7, 1171.

16 (a) B.-H. Ye, M.-L. Tong and X.-M. Chen, *Coord. Chem. Rev.*, 2005, 249, 545; (b) J. Yang, Q. Yue, J.-D. Li, J.-J. Cao, G.-H. Li and J.-S. Chen, *Inorg. Chem.*, 2006, 45, 2857; (c) J. Yao, W. Huang, B. Li, S. Gou and Y. Xu, Inorg. *Chem. Commun*., 2002, 5, 711; (d) S. Dalai, P. S. Mukherjee, G. Rogez, T. Mallah, M. G. B. Drew and N. R. Chaudhuri, *Eur. J. Inorg. Chem.*, 2002, 31, 3292; (e) M. Eddaoudi, D. B. Moler, H. Li, B. Chen, T. M. Reineke, M. O'Keeffe and O. M. Yaghi, *Acc. Chem. Res.*, 2001, 34, 319; (f) G. Férey, C. Serre, C. Mellot-Draznieks and F. Millange, *Acc. Chem. Res.*, 2005, 38, 217.

17 (a) V. A. Blatov, *IUCr CompComm Newsletter*, 2006, 7, 4; (b) V. A. Blatov, A. P. Shevchenko and V. N. Serezhkin, *J. Appl. Crystallogr.*, 2000, 33, 1193; (c) V. A. Blatov, M. O' Keeffe and D. M. Proserpio, *CrystEngComm*, 2010, 12, 44, see also, ***http://www.topos.ssu.Samara.ru.***

18 O. D. Friedrichs, Program SYSTRE 1.14 beta ***http://gavrog.***sourceforge.net/, 2007.

19 *Bruker. SMART*, *SAINT and SADABS*, Bruker AXS Inc., Madison, Wisconsin, USA, 1998.

20 G. M. Sheldrick, SHELXTL NT, version 5.1, Program for Solution and Refinement of Crystal Structures, University of GÖttingen, GÖttingen, Germany, 1997.

21 Bruker 2000, SMART, version 5.0, SAINT-plus version 6, SHELXTL, version 6.1, and SADABS version 2.03, Bruker AXS Inc.: Madison, WI.

22 A. L. Spek, *Implemented as the PLATON Procedure*, *a Multipurpose Crystallographic Tool*, Utrecht University, Utrecht, The Netherlands, 1998.

23 (a) J. S. Hu, L. F. Huang, X. Q. Yao, L. Qin, Y. Z. Li, Z. J. Guo, H. G. Zheng, Z. L. Xue, *Inorg. Chem.*, 2011, 50, 2404; (b) P. Alborés, E. Rentschler, *DaltonTrans.*, 2009,2609; (b) J. L. Song, H. H. Zhao, J. G. Mao, K. R. Dunbar, *Chem. Mater.*,

2004, 16, 1884.

24 (a) A. L. Spek, *J. Appl. Crystallogr.*, 2003, 36, 7; (b) A. L. Spek, *PLATON, A Multipurpose Crystallographic Tool*, Utrecht University, Utrecht, The Netherlands, 2002.

25 (a) X. Zhang, L. Fan, W. Zhang, Y. Ding, W. Fan and X. Zhao, *Dalton Trans.*, 2013, 42, 16562; (b) X. J. Liang, X. D. Chen and J. C. Zhao, *Chem. Soc. Rev.*, 2014, 43, 473; (c) H. Fu, Y. G. Li, Y. Liu, W. L. Chen, Q. Wu, J. X. Meng, X. L. Wang, Z. M. Zhang and E. B. Wang, *Cryst. Growth Des.*, 2011, 11, 458; (d) W. Wang, J. Yang, W. Q. Kan and J. F. Ma, *CrystEngComm*, 2013, 15, 5844.

26 X. L. Wang, X. T. Sha, G. C. Liu, N. L. Chen, *CrystEngComm*, 2015, 17, 7290.

27 J. Lü, J. X. Lin, X. L. Zhao and R. Cao, *Chem. Commun.*, 2012, 48, 669.

28 X. L. Wang, C. H. Gong, J. W. Zhang, G. C. Liu, X. M. Kan and N. Xu, *CrystEngComm*, 2015, 17, 4179.

29 A. K. Paul, R. Karthik, S. Natarajan, *Cryst. Growth Des.*, 2011, 11, 5741.

30 H. Lin, P. A. Maggard, *Inorg. Chem.*, 2008, 47, 8044.

31 (a) K. Y. Cui, F. Y. Li, L. Xu, Y. C. Wang, Z. X. Sun and H. G. Fu, *CrystEngComm*, 2013, 15, 4721; (b) Z. Zhang, J. Yang, Y. Y. Liu and J. F. Ma, *CrystEngComm*, 2013, 15, 3843; (c) W. Q. Kan, J. Yang, Y. Y. Liu and J. F. Ma, *Dalton Trans.*, 2013, 42, 3843.

32 X. Wang, C. Gong, J. Zhang, G. Liu, X. Kan and N. Xu, *CrystEngComm*, 2015, 17, 4179.

33 X. T. Zhang, L. M. Fan, W. Zhang, Y. S. Ding, W. L. Fan and X. Zhao, *Dalton Trans.*, 2013, 42, 16562.

34 Y. Li, J. Niu, L. Yin, W. Wang, Y. Bao, J. Chen, Y. Duan, *J. Environ. Sci.*, 2011, 23, 1911.

35 (a) Y. Q. Chen, S. J. Liu, Y. W. Li, G. R. Li, K. H. He, Y. K. Qu, T. L. Hu and X. H. Bu, *Cryst. Growth Des.*, 2012, 12, 5426; (b) J. X. Meng, Y. Lu, Y. G. Li, H. Fu and E. B. Wang, *CrystEngComm*, 2011, 13, 2479; (c) J. Guo, J. Yang, Y. Y. Liu and J. F. Ma, *CrystEngComm*, 2012, 14, 6609; (d) H. X. Yang, T. F. Liu, M. N. Cao, H. F. Li, S. Y. Gao and R. Cao, *Chem. Commun.*, 2010, 46, 2429.

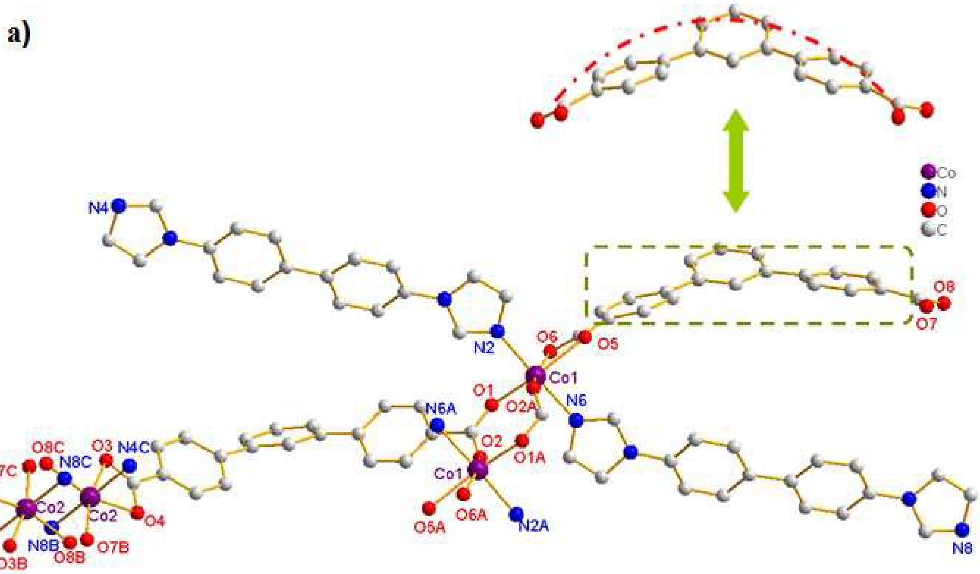

Fig. 1 (a) Coordination environment of the Co^{II} ion in complex **1** (Symmetry codes: A: -x + 1, -y, -z + 1; B: x + 1, -y + 1/2, z + 1/2; C: -x + 1, y + 1/2, -z + 1/2; D: x, -y + 1/2, z - 1/2).

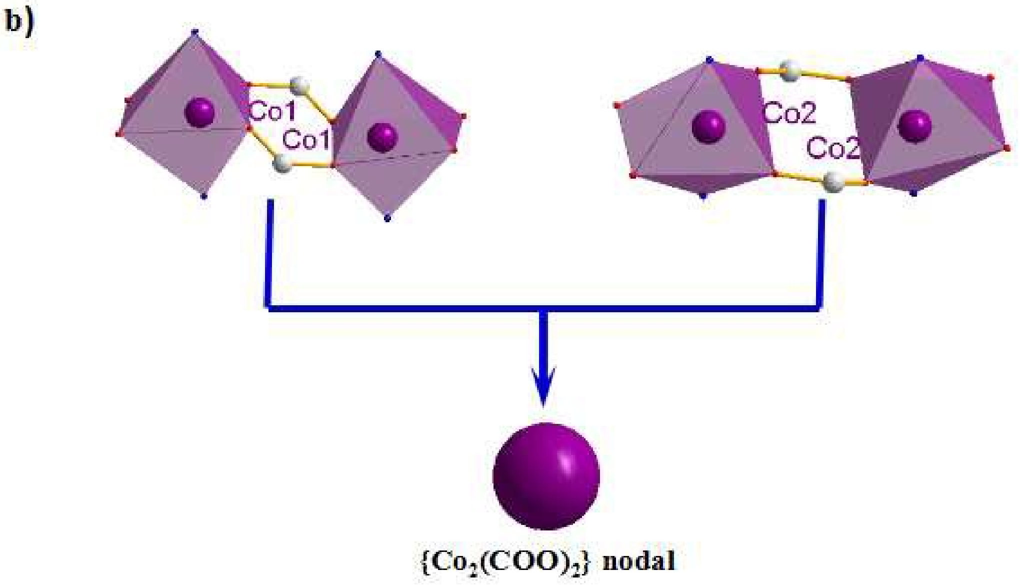

Fig. 1 (b) The two binuclear {Co$_2$(COO)$_2$} SBUs.

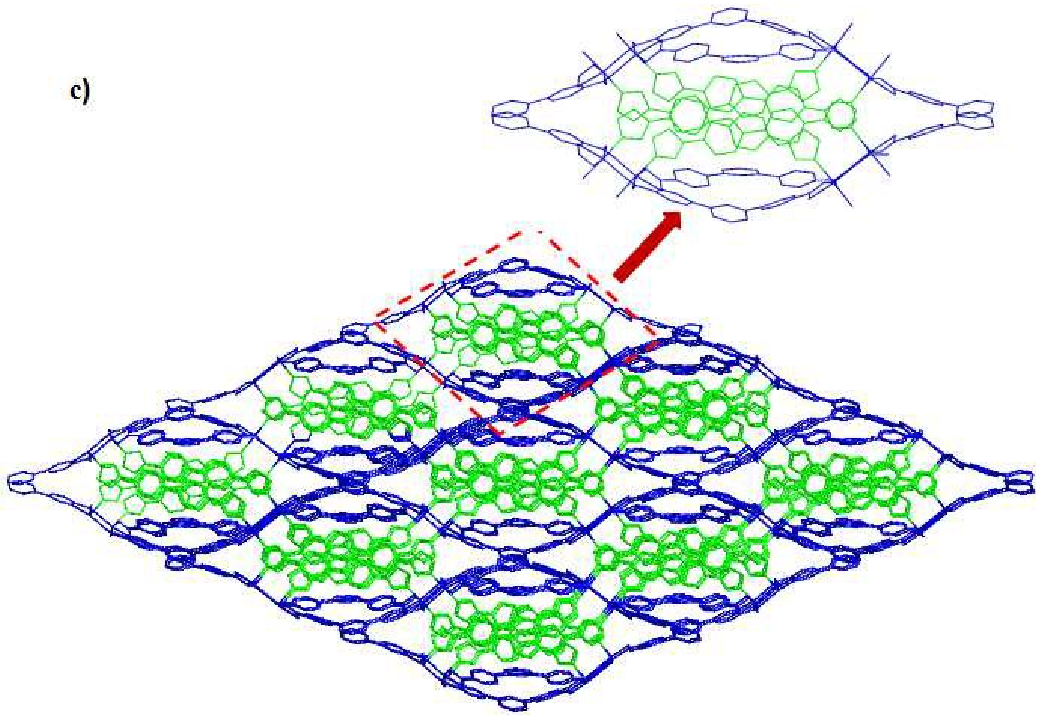

Fig. 1 (c) The 3D structure frameworks of complex **1** (blue chain: dpb^{2-} ligands; green chain: 4,4′-bibp ligands).

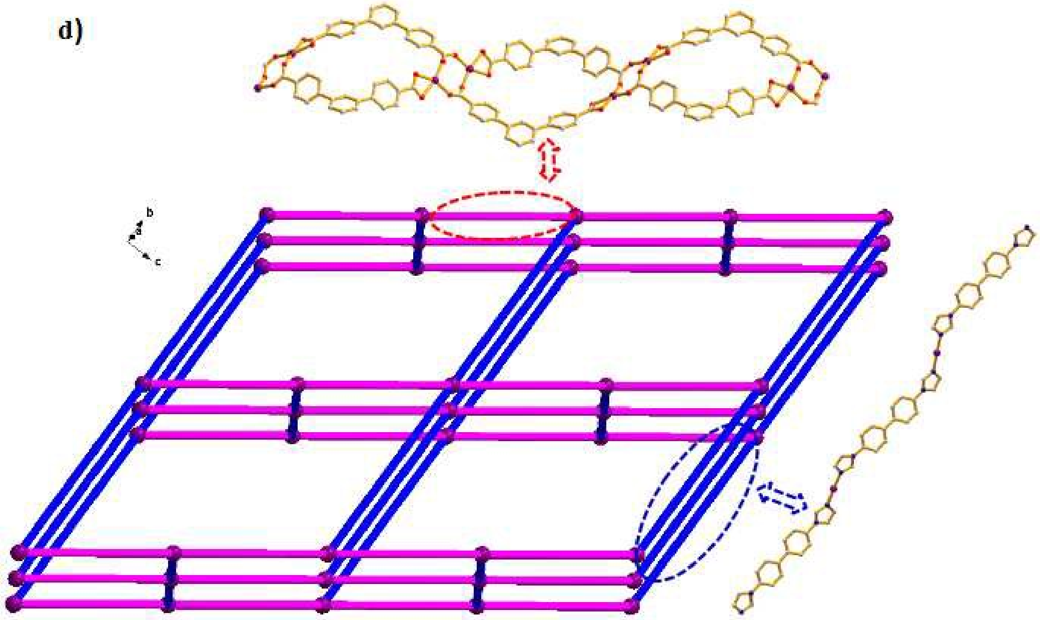

Fig. 1 (d) The 3D 4-connected **cds** topology with the Schläfli symbol (6^5·8) in complex **1**.

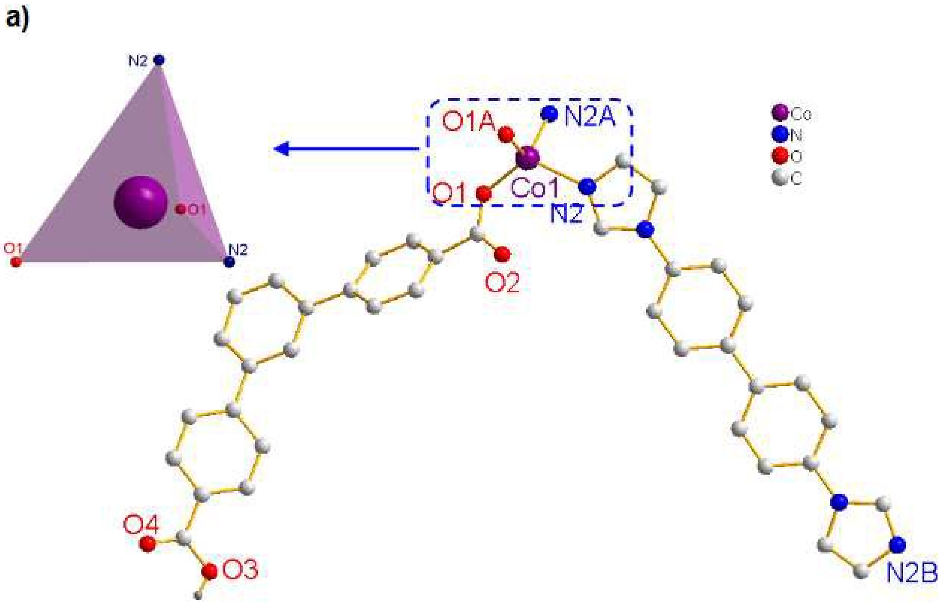

Fig. 2 (a) Coordination environment of the Co^{II} ion in complex **2** (Symmetry codes: A: -x + 1, y, -z + 3/2; B: -x + 3/2, -y + 5/2, -z + 2).

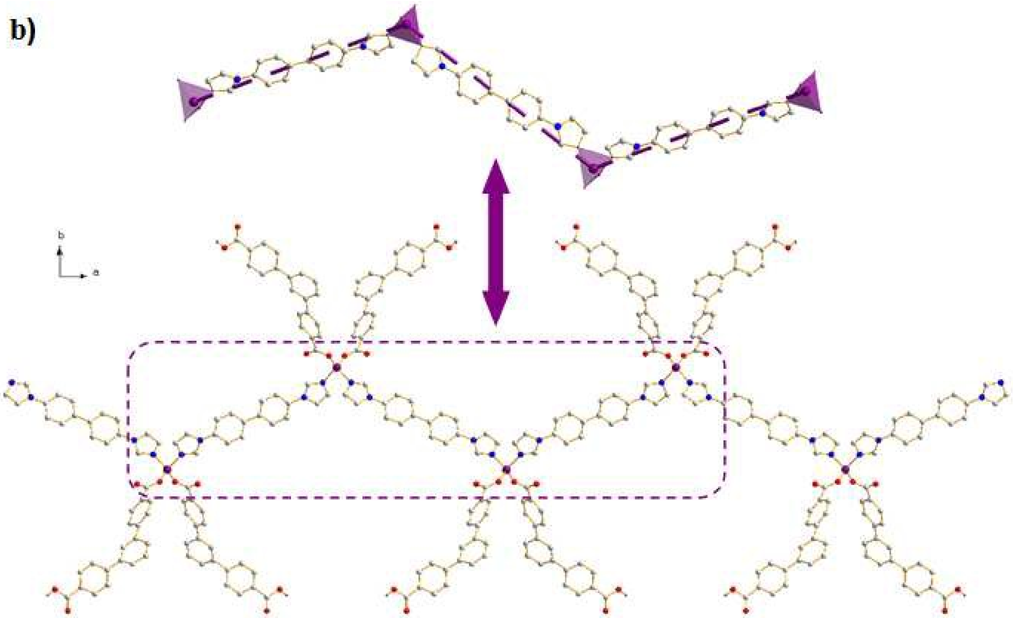

Fig. 2 (b) The simplified 1D zigzag chain structure of along the a axis in complex **2**.

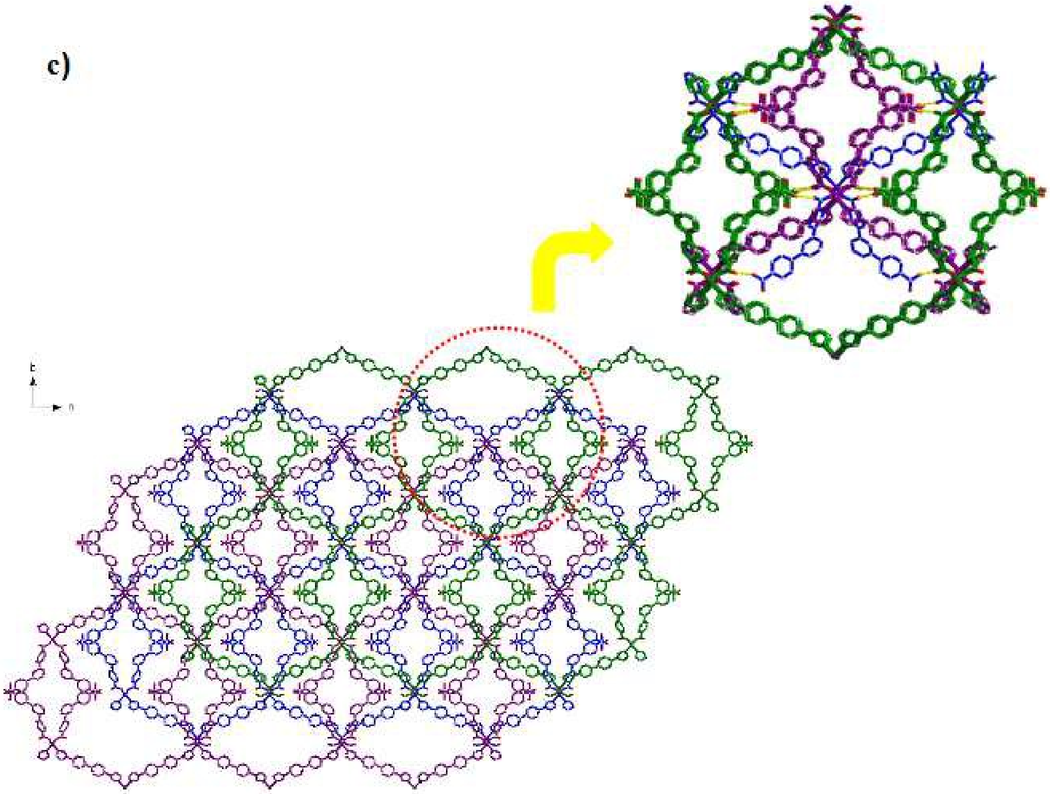

Fig. 2 (c) From 1D chain to 3D supramolecular structure of complex **2**, which are linked by O-H···O hydrogen bonds along [1,1,0] orientation (the yellow dotted line represents O-H···O hydrogen bonds).

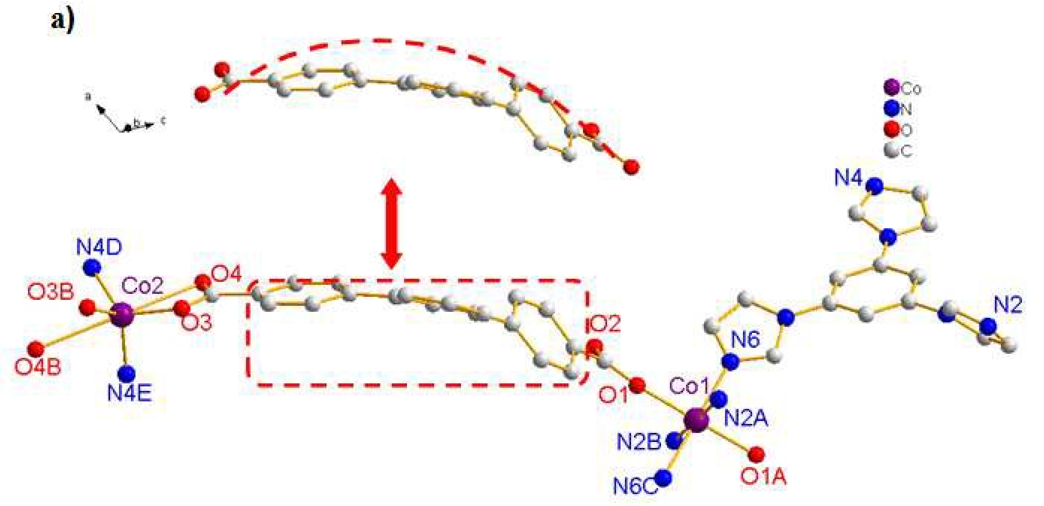

Fig. 3 (a) Coordination environment of the Co^{II} ion in complex **3** (Symmetry codes: A: -x + 3/2, -y + 1/2, -z + 1; B: x, y + 1, z - 1; C: -x + 1, y, -z + 1/2; D: x, y - 1, z + 1).

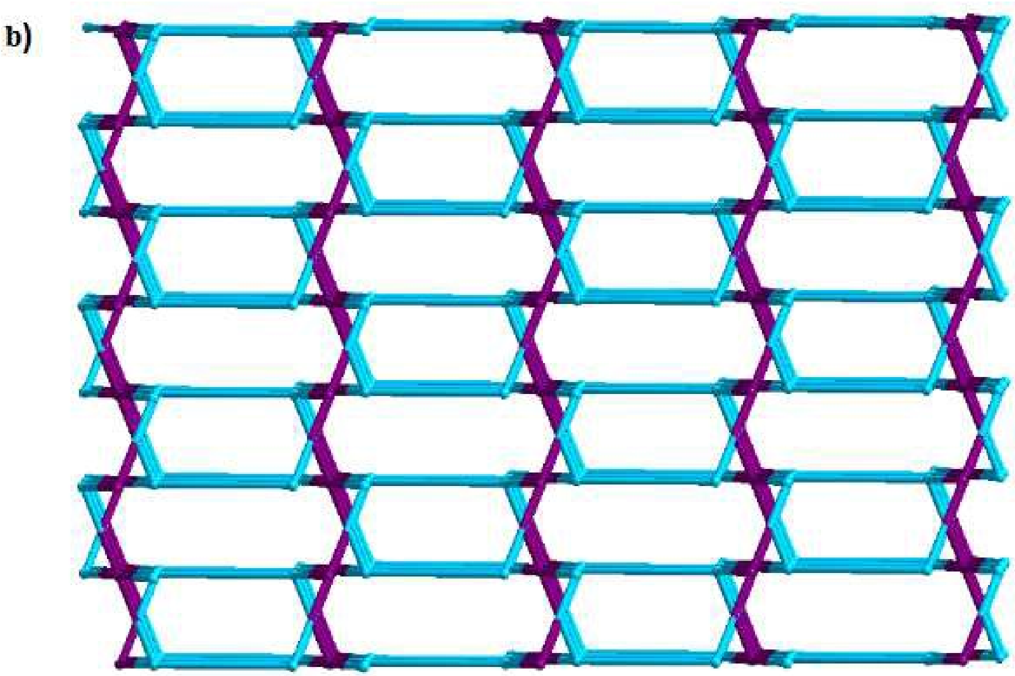

Fig. 3 (b) The unprecedented (3,4)-connected $[Co(tib)_2]_n^{2n+}$ frameworks with $(6^2\cdot8^2\cdot10^2)(6^2\cdot8)^2$ topology (blue spheres: tib ligands; violet spheres: Co^{II} atoms).

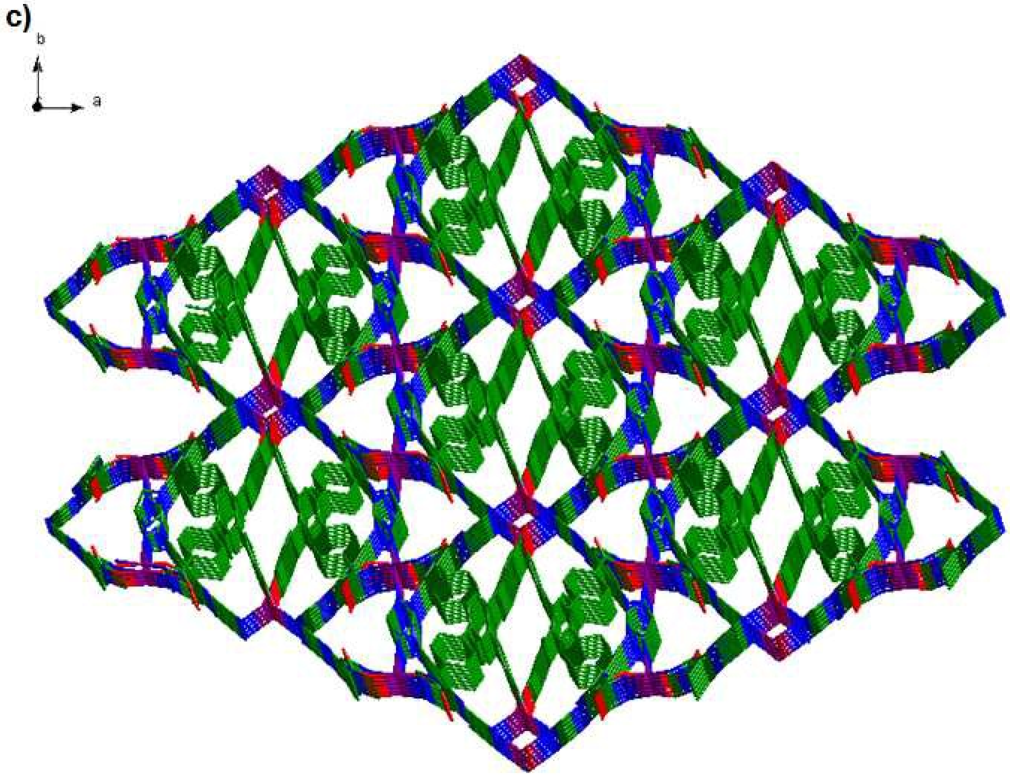

Fig. 3 (c) The 3D structure frameworks of complex **3** (green spheres: C atoms).

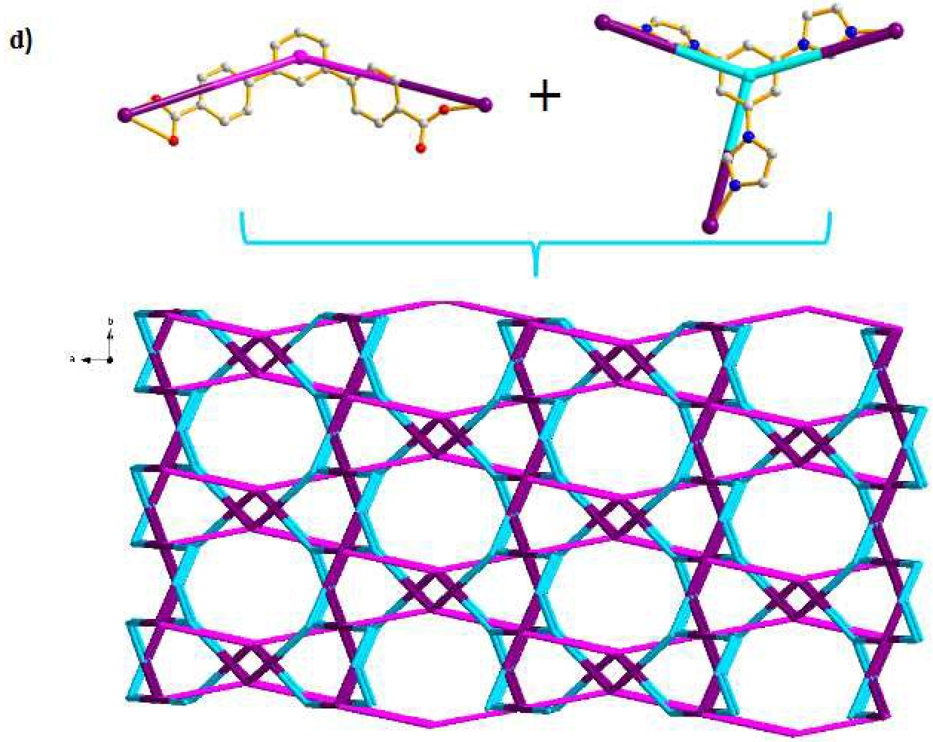

Fig. 3 (d) Views of the (3,4,6)-connected frameworks with unprecedented $(6^2,7)^2(6^4\cdot7^5\cdot8^4\cdot9\cdot10)(6^4\cdot8^2)$ topology (blue spheres: tib ligands; violet spheres: Co^{II} atoms; pink bonds: dpb^{2-} ligands).

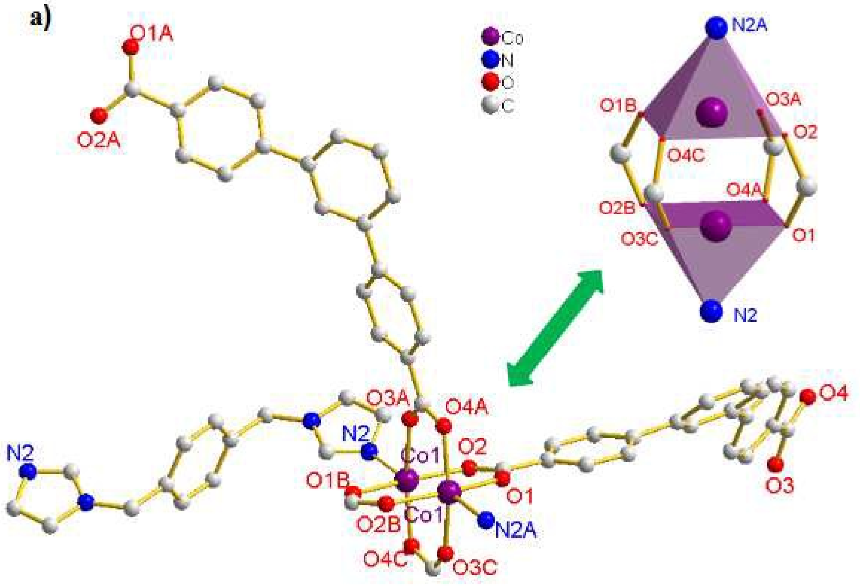

Fig. 4 (a) Coordination environment of the Co^{II} ion in complex **4** (Symmetry codes: A: -x + 3/2, -y + 3/2, -z + 1; B:-x + 1, y, -z + 1/2; C: -x + 1, y - 1, -z + 1/2; D: -x + 1, -y - 1, -z + 1).

b)

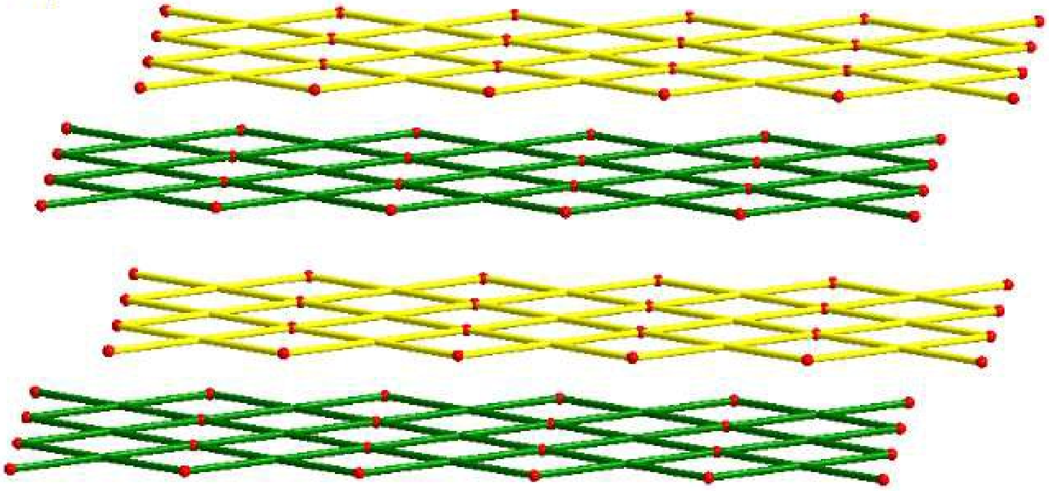

Fig. 4 (b) The 4-connected **sql** $[Co(dpb)_2]_n^{2n+}$ sheet with $(4^4 \cdot 6^2)$ topology.

c)

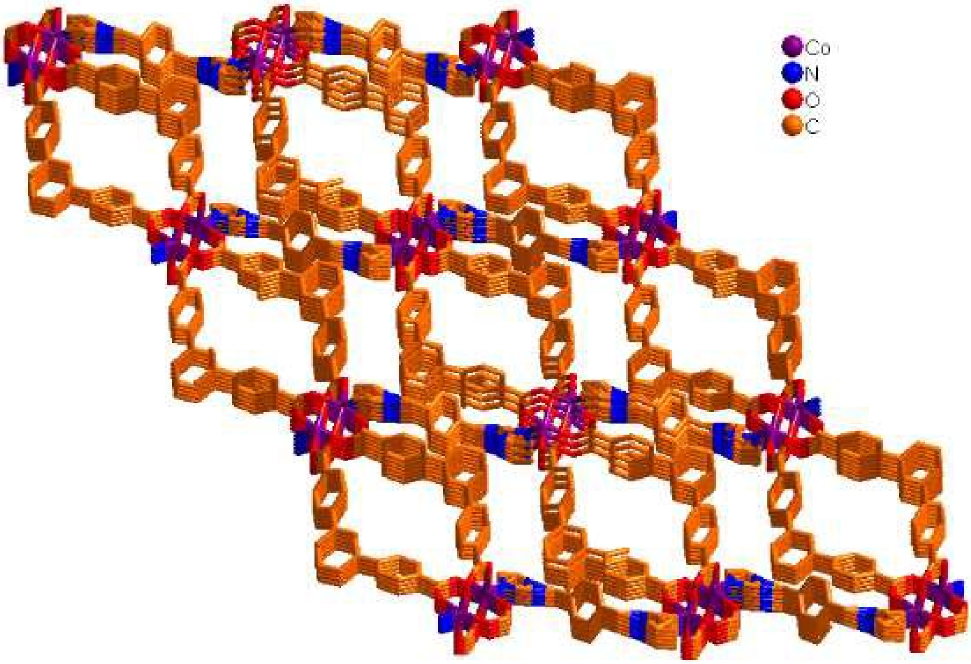

Fig. 4 (c) The 3D structure frameworks of complex **4**.

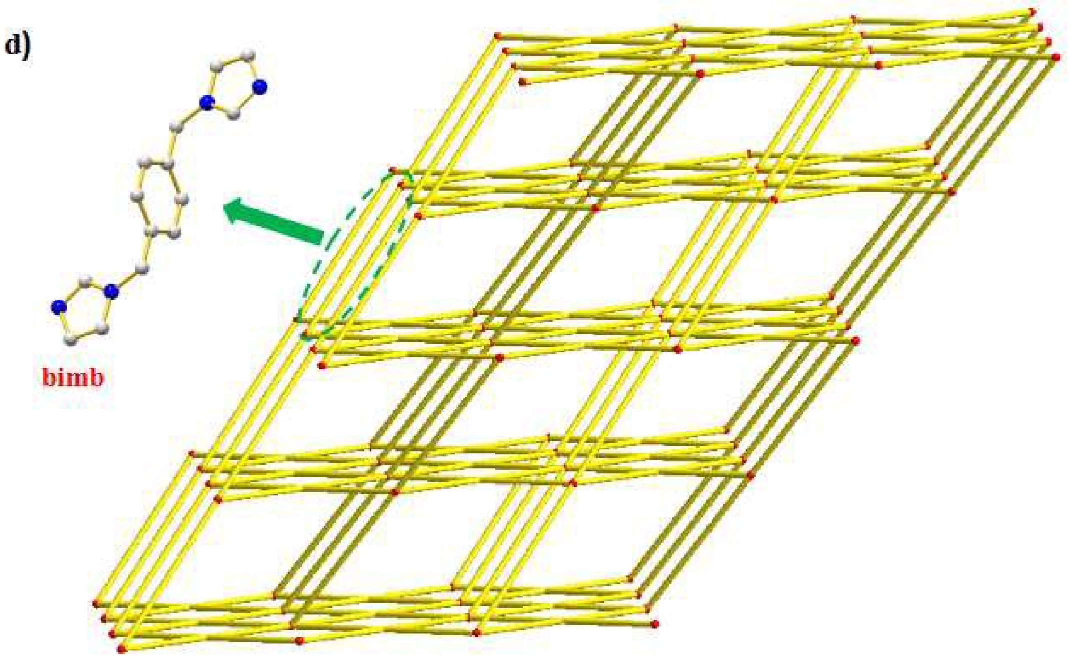

Fig. 4 (d) Views of the unprecedented 6-connected frameworks with ($4^4 \cdot 6^{11}$) topology.

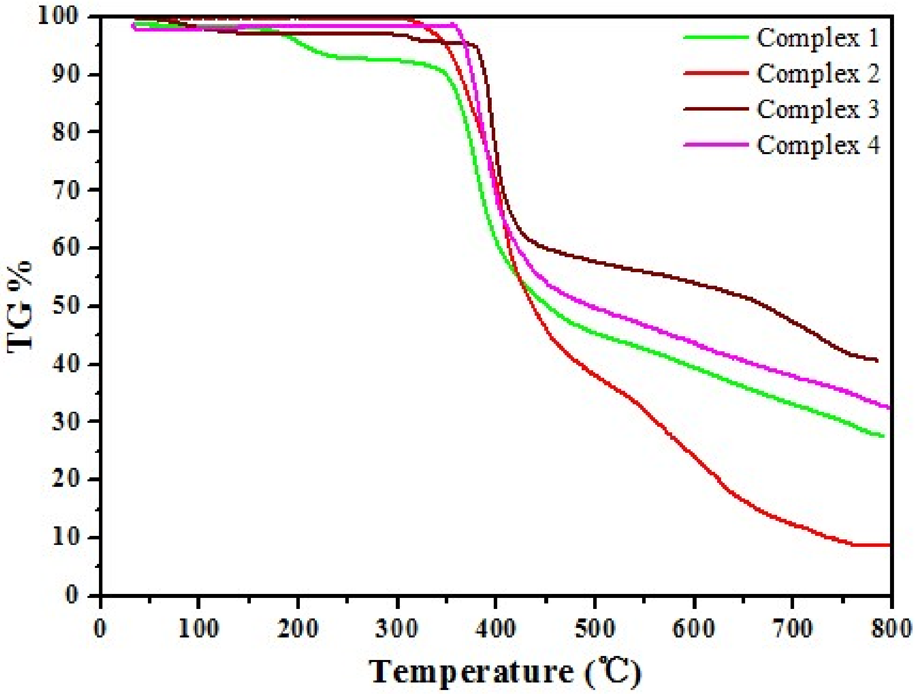

Fig. 5 The TGA curves for complexes **1**-**4**.

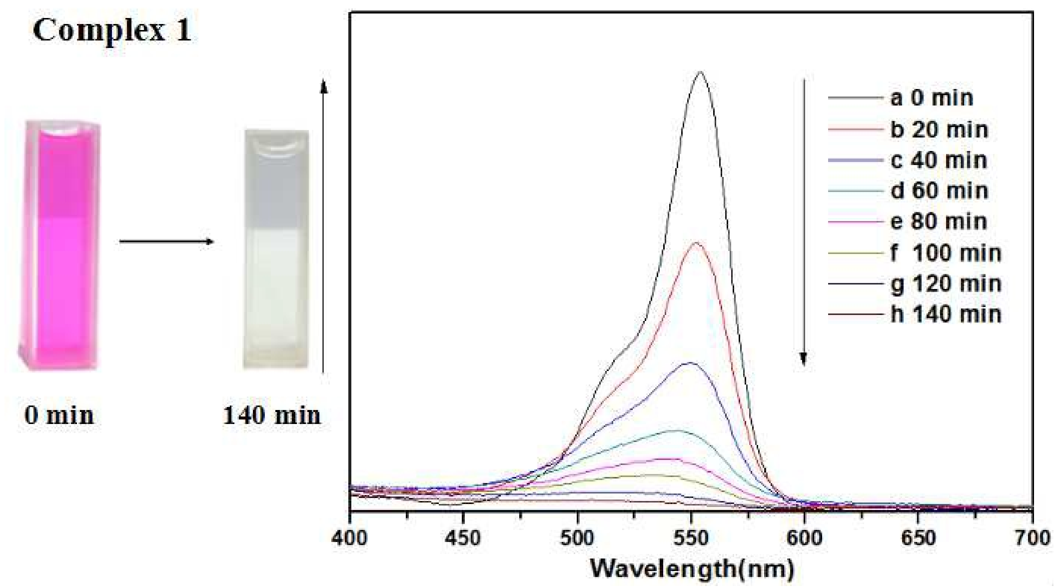

Fig. 6 (a) Absorption spectra of the RhB solution in the presence of complex **1**. Left: color change photograph of dye solutions in 0 min and 140 min.

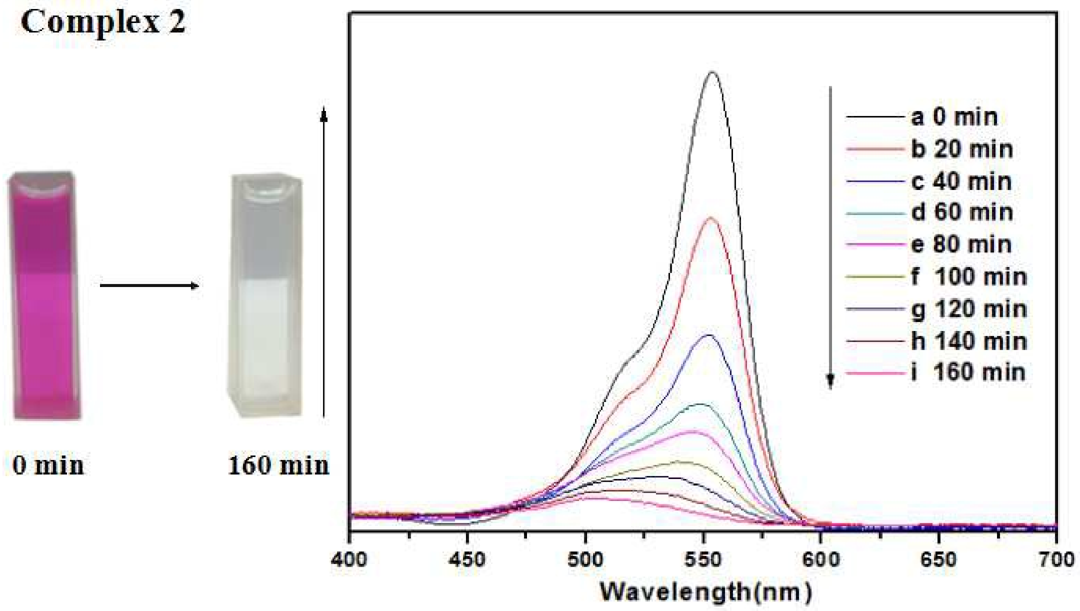

Fig. 6 (b) Absorption spectra of the RhB solution in the presence of complex **2**. Left: color change photograph of dye solutions in 0 min and 160 min.

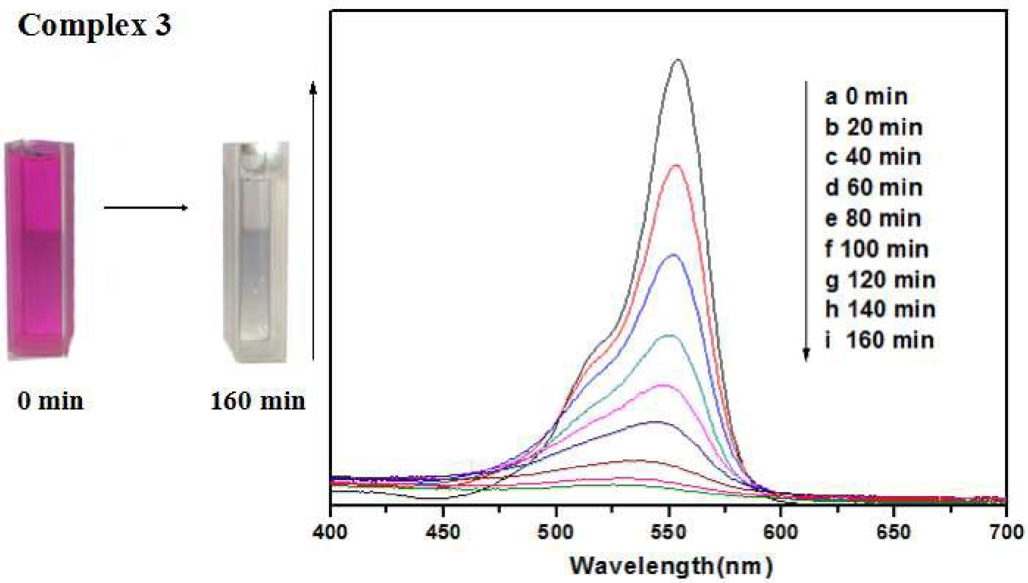

Fig. 6 (c) Absorption spectra of the RhB solution in the presence of complex **3**. Left: color change photograph of dye solutions in 0 min and 160 min.

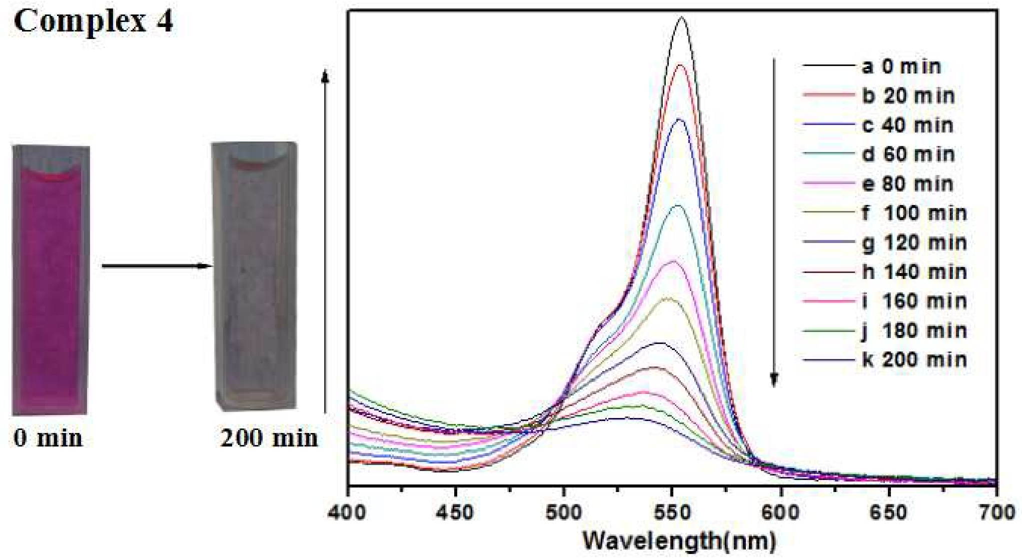

Fig. 6 (d) Absorption spectra of the RhB solution in the presence of complex **4**. Left: color change photograph of dye solutions in 0 min and 200 min.

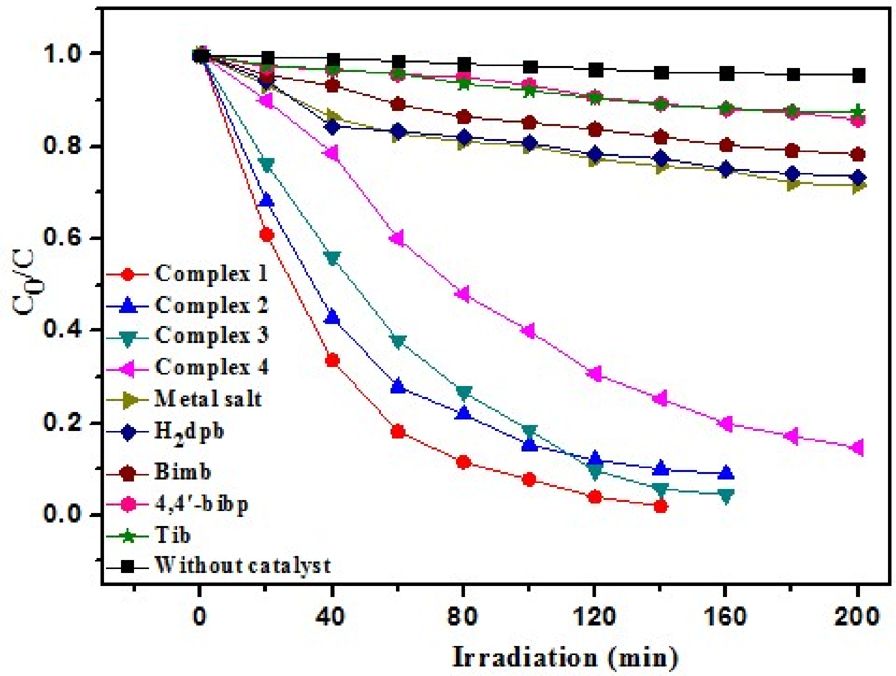

Fig. 6 (e) Plots of concentration ratios of RhB (c_0/c) against irradiation time (min) in the presence of complexes **1-4**, ligands, metal salt and without any catalyst during the decomposition reaction under UV irradiation.

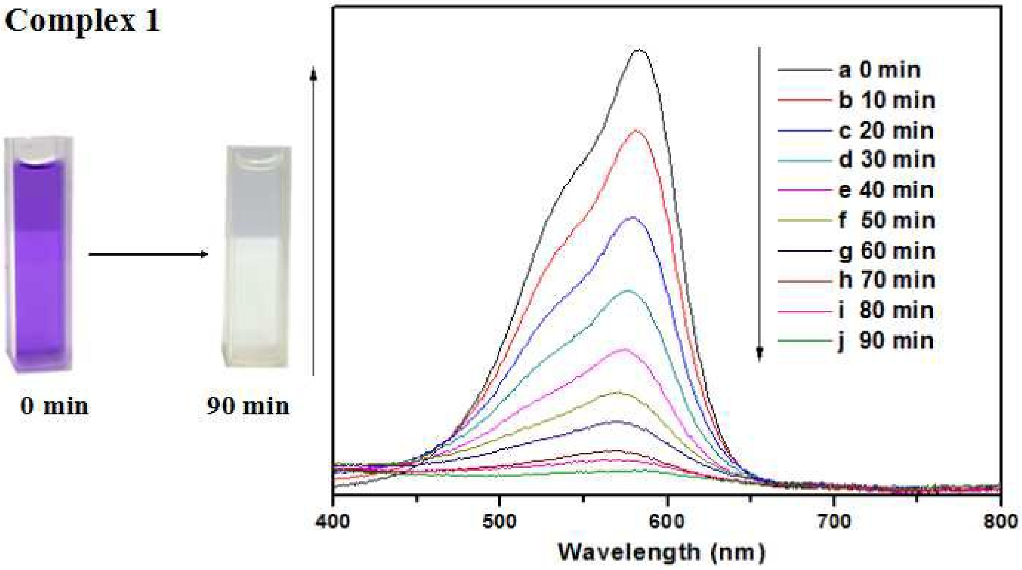

Fig. 7 (a) Absorption spectra of the MV solution in the presence of complex **1**. Left: color change photograph of dye solutions in 0 min and 90 min.

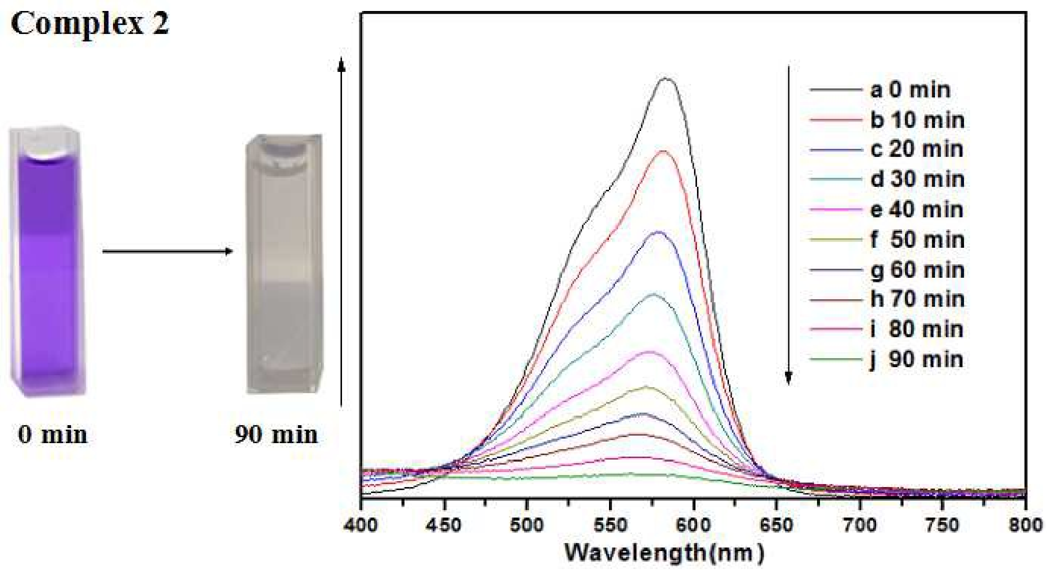

Fig. 7 (b) Absorption spectra of the MV solution in the presence of complex **2**. Left: color change photograph of dye solutions in 0 min and 90 min.

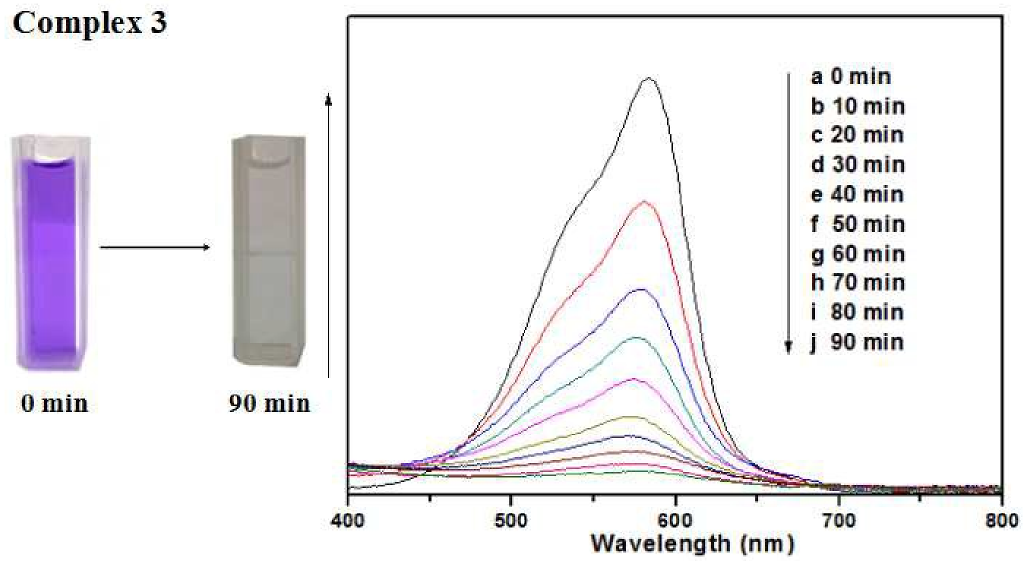

Fig. 7 (c) Absorption spectra of the MV solution in the presence of complex **3**. Left: color change photograph of dye solutions in 0 min and 90 min.

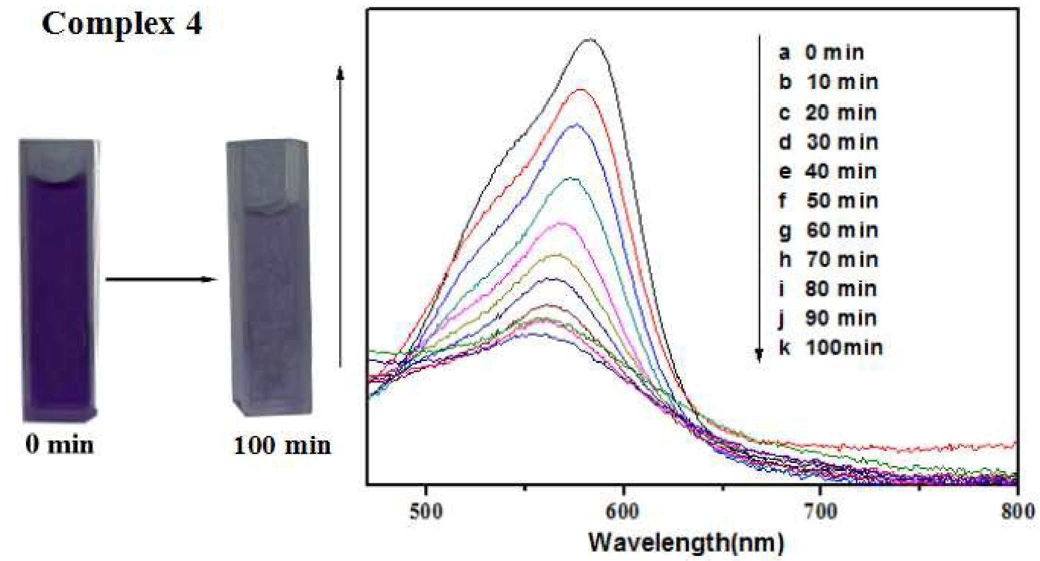

Fig. 7 (d) Absorption spectra of the MV solution in the presence of complex **4**. Left: color change photograph of dye solutions in 0 min and 100 min.

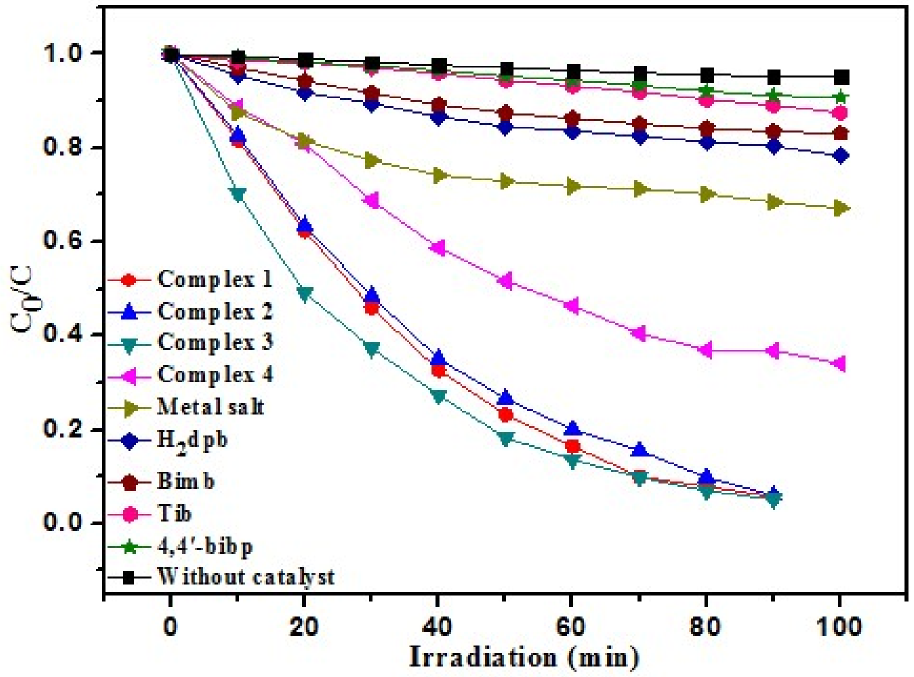

Fig. 7 (e) Plots of concentration ratios of MV (c_0/c) against irradiation time (min) in the presence of complexes **1-4**, ligands, metal salt and without any catalyst during the decomposition reaction under UV irradiation.

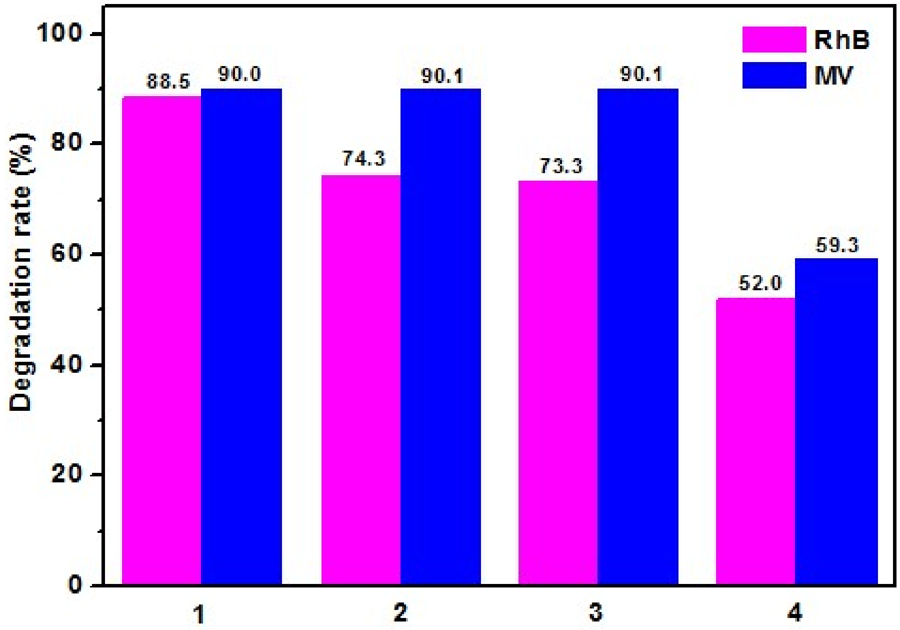

Fig. 8 Degradation rates of the RhB and MV solutions in the presence of complexes **1-4**.

Table 1 Summary of crystal data and structure refinement parameters for **1-4**

Compound	**1**	**2**	**3**	**4**
Empirical formula	$C_{80}H_{58}Co_2N_{10}O_8$	$C_{58}H_{40}C_oNO_8$	$C_{70}H_{52}Co_2N_{12}O_{10}$	$C_{63}H_{59}Co_2N_7O_{11}$
Formula weight	1405.22	979.87	1339.10	1208.03
Crystal system	Monoclinic	Monoclinic	Monoclinic	Monoclinic
Space group	$P2_1$/c	$C2$/c	$C2$/c	$C2$/c
a (Å)	32.836(3)	33.193(3)	32.800(3)	27.805(3)
b (Å)	14.4409(13)	6.8956(6)	12.5860(11)	9.3810(9)
c (Å)	14.2280(12)	21.9291(19)	16.0471(14)	24.923(2)
α (°)	90	90	90	90
β (°)	101.308(2)	114.468(2)	116.928(3)	114.715(3)
γ(°)	90	90	90	90
V (Å^3)	6615.7(10)	4568.5(7)	5906.4(9)	5905.5(9)
Z	4	4	4	4
D_{calcd}(Mg m^{-3})	1.411	1.425	1.506	1.359
μ (mm^{-1})	0.570	0.441	0.638	0.628
Reflections collected	33145	11076	14741	14379
Data/parameters	11655 /903	4032 /321	5205 /426	5194 / 428
F(000)	2904	2028	2760	2512
T (K)	298(2)	298(2)	298(2)	298(2)
R_{int}	0.0899	0.1498	0.0518	0.0638
Final R indices [$I > 2\sigma(I)$]	$R_1 = 0.0774$	$R_1 = 0.0757$	$R_1 = 0.0492$	$R_1 = 0.0603$
	$wR_2 = 0.1816$	$wR_2 = 0.1402$	$wR_2 = 0.1045$	$wR_2 = 0.1624$
R indices (all data)	$R_1 = 0.1692$	$R_1 = 0.1471$	$R_1 = 0.0844$	$R_1 = 0.1126$
	$wR_2 = 0.2048$	$wR_2 = 0.1589$	$wR_2 = 0.1122$	$wR_2 = 0.1937$
Gof	1.030	1.045	1.066	1.044

[a] $R_1 = \Sigma\|F_o| - |F_c\|/\Sigma|F_o|$, $wR_2 = [\Sigma w(F_o^2 - F_c^2)^2]/[\Sigma w(F_o^2)^2]^{1/2}$.

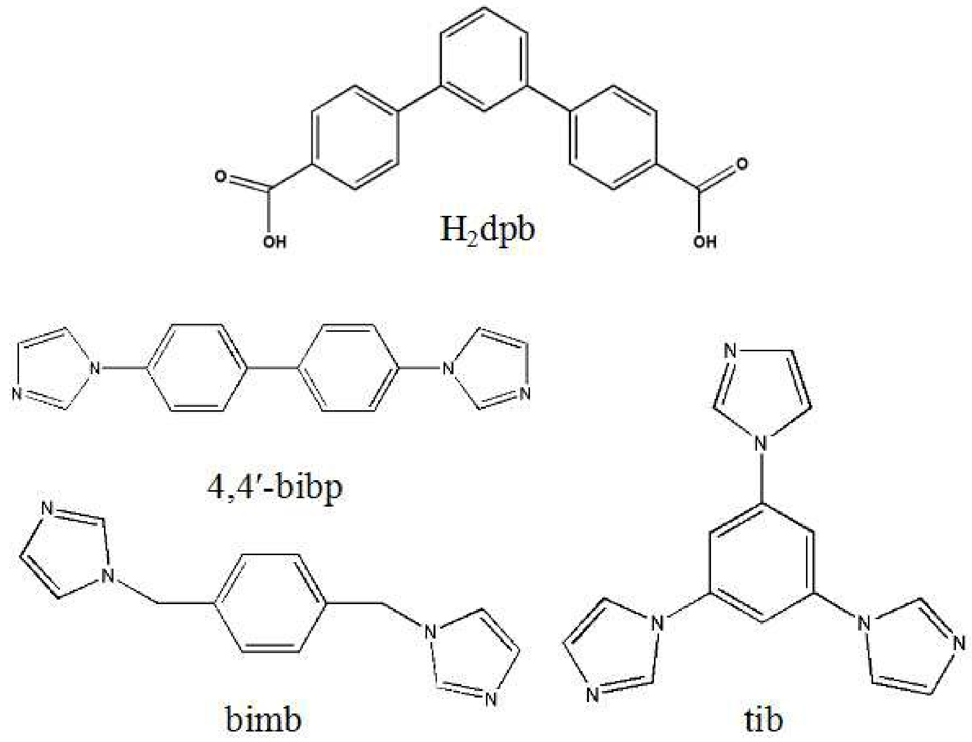

Scheme 1 Structures of H$_2$dpb and three auxiliary N-donor bridging linkers.

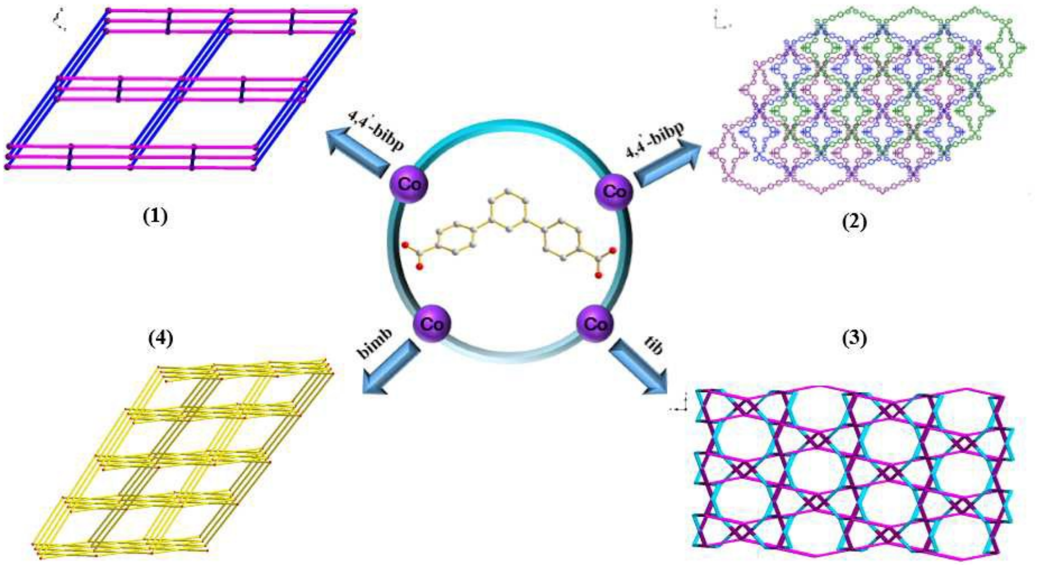

Scheme 2 Various polymeric structures of complexes **1**-**4**.

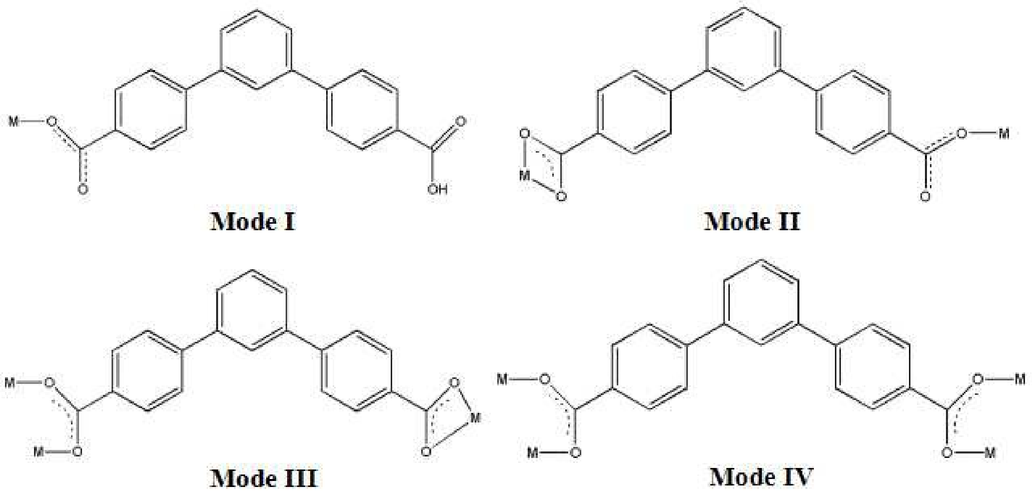

Scheme 3 Diverse coordination modes of H_2dpb in complexes **1−4**.

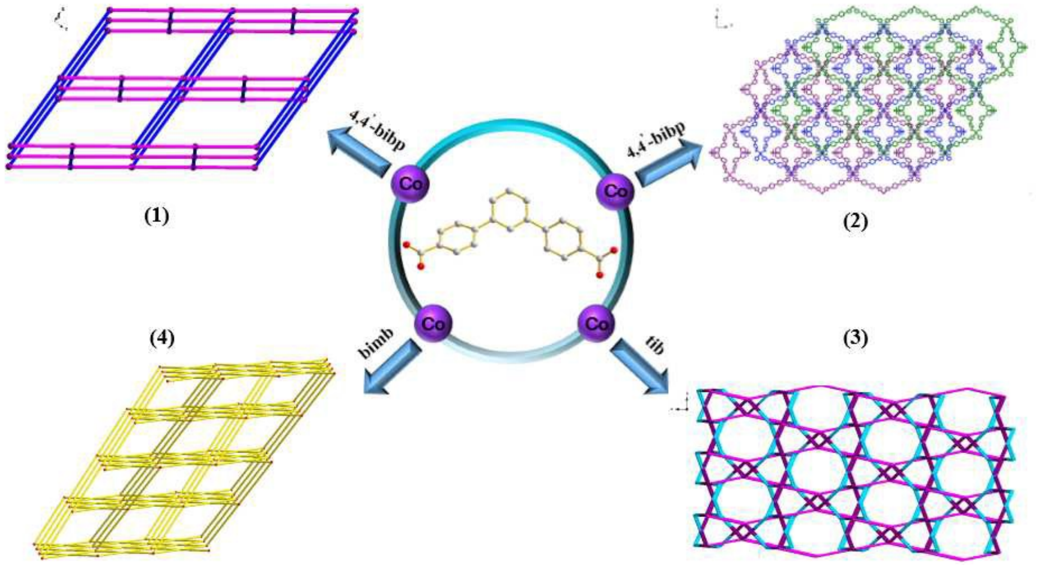

Various polymeric structures of complexes **1-4**.